الجامعة التكنولوجية

قسم الهندسة الكيمياوية

المرحلة الاولى

فيزياء البيئة

أ.م . د . فـلـك اسـامـة

Environmental physics:

By dr. falak O. Abas

Essential of environmental physics:

Physics has always been concerned with understanding the natural environment, and, in its early days, was often referred to as ―Natural Philosophy." Environmental Physics, as we choose to define it, is the measurement and analysis of interactions between organisms and their environments.

To grow and reproduce successfully, organisms must come to terms with the state of their environment. Some microorganisms can grow at temperatures between −6 and 120 ◦C and, when they are desiccated, can survive even down to −272 ◦C.

Higher forms of life on the other hand have adapted to a relatively narrow range of environments by evolving sensitive physiological responses to external physical stimuli. When environments change, for example because of natural variation or because of human activity, organisms may, or may not, have sufficiently flexible responses to survive.

The physical environment of plants and animals has five main components which determine the survival of the species:

(i) The environment is a source of radiant energy which is trapped by the process of photosynthesis in green cells and stored in the form of carbohydrates, proteins, and fats. These materials are the primary source of metabolic energy for all forms of life on land and in the oceans;

(ii) The environment is a source of the water, carbon, nitrogen, other minerals, and trace elements needed to form the components of living cells;

(iii) factors such as temperature and day length determine the rates at which plants grow and develop, the demand of animals for food, and the onset of reproductive cycles in both plants and animals;

(iv) The environment provides stimuli, notably in the form of light or gravity, which are perceived by plants and animals and provide frames of reference both in time and in space. These stimuli are essential for resetting biological clocks, providing a sense of balance, etc.;

(v) The environment determines the distribution and viability of pathogens and parasites which attack living organisms, and the susceptibility of organisms to attack.

To understand and explore relationships between organisms and their environment, the biologist should be familiar with the main concepts of the environmental sciences. He or she must search for links between physiology, biochemistry, and molecular biology on the one hand and atmospheric science, soil science, and hydrology on the other. One of these links is environmental physics. The presence of an organism modifies the environment to which it is exposed, so that the physical stimulus received *from* the environment is partly determined by the physiological response *to* the environment. When an organism interacts with its environment, the physical processes involved are rarely simple and the physiological mechanisms are often imperfectly understood.

Fortunately, physicists are trained to use Occam's Razor when they interpret natural phenomena in terms of cause and effect: i.e. they observe the behavior of a system and then seek the simplest way of describing it in terms of governing variables. Boyle's Law and Newton's Laws ofMotion are classic examples of this attitude. More complex relations are avoided until theweight of experimental evidence shows they are essential. Many of the equations discussed in this book are approximations to reality which have been found useful to establish and explore ideas. The art of environmental physics lies in choosing robust approximations which maintain the principles of conservation for mass, momentum, and energy.

Properties of Gases and Liquids

The physical properties of gases influence many of the exchanges that take place between organisms and their environment. The relevant equations for air therefore form an appropriate starting point for an environmental physics text. They also provide a basis for discussing the behavior of water vapor, a gas whose significance in meteorology, hydrology, and ecology is out of all proportion to its relatively small concentration in the atmosphere. Because the evaporation of water from soils, plants, and animals is also an important process in environmental physics, this chapter reviews the principles by which the state of liquid water can be described in organisms and soil, and by which exchange occurs between liquid and vapor phases of water.

Gases and Water Vapor

Pressure, Volume, and Temperature

The observable properties of a gas such as temperature and pressure can be related to the mass and velocity of its constituent molecules by the Kinetic Theory of Gases which is based on Newton's Laws of Motion. Newton established the principle that when force is applied to a body, its momentum, the product of mass and velocity, changes at a rate proportional to the magnitude of the force. Appropriately, the unit of force in the Système Internationale is the Newton and the unit of pressure (force per unit area) is the Pascal—from the name of another famous natural philosopher.

The pressure p which a gas exerts on the surface of a liquid or solid is a measure of the rate at which momentum is transferred to the surface from molecules which strike it and rebound. Assuming that the kinetic energy of all the molecules in an enclosed space is constant and by making further assumptions about the nature of a *perfect* gas, a simple relation can be established between pressure and kinetic energy per unit volume. When the density of the gas is ρ and the mean square molecular velocity is $v2$, the kinetic energy per unit volume is $\rho v2/2$ and Equation (2.3), which is a statement of the *Ideal Gas Law*, is sometimes used in the Form

$$p = \rho R T / M$$

Obtained by writing the density of a gas as its molecular mass divided by its molecular volume, i.e.

$$\rho = M/V_{\mathrm{m}}.$$

For unit mass of any gas with volume V, $\rho = 1/V$ so Eq. (2.5) can also be written in the form

$$pV = RT/M.$$

Equation (2.7) provides a general basis for exploring the relation between pressure, volume, and temperature in unit mass of gas and is particularly useful in four cases:

1. Constant volume—p proportional to T,

2. Constant pressure (isobaric)—V proportional to T,

3. Constant temperature (isothermal)—V inversely proportional to p,

4. Constant energy (adiabatic)—p, V, and T may all change.

When the molecular weight of a gas is known, its density at STP can be calculated from Eq. (2.6) and its density at any other temperature and pressure from Eq. (2.5). Table 2.1 contains the molecular weights and densities at STP of the main constituents of dry air. Multiplying each density by the appropriate volume fraction gives the mass concentration of each component and the sum of these concentrations is the density of dry air. From a density of 1.292 kg m−3 and from Eq. (2.5) the effective molecular weight of dry air (in g) is 28.96 or 29 within 0.1%.

Since air is a mixture of gases, it obeys Dalton's Law, which states that the total pressure of a mixture of gases that do not react with each other is given by the sum of the partial pressures. *Partial pressure* is the pressure that a gas would exert at the same temperature as the mixture if it alone occupied the volume that the mixture occupies.

Water Vapor and its Specification

The evaporation of water at the earth's surface to form water vapor in the atmosphere is a process of major physical and biological importance because the latent heat of vaporization is large in relation to the specific heat of air. The heat released by condensing 1 g of water vapor is enough to raise the temperature of 1 kg of air by 2.5 K. Water vapor has been called the ―working substance" of the atmospheric heat engine because of its role in global heat transport. The total mass of water vapor in the air at any moment is enough to supply only 1 week of the world's precipitation, so the process of evaporation must be very efficient in replenishing the atmospheric reservoir. On a much smaller scale, it is the amount of latent heat removed by the evaporation of sweat that allows man and many other mammals to survive in hot climates. Sections which follow describe the physical significance of different ways of specifying the amount of vapor in a sample of air and relations between them.

Transport of Heat, Mass, and Momentum

The last chapter was concerned primarily with ways of specifying the state of the atmosphere in terms of properties such as pressure, temperature, and gas concentration.

To continue this introduction to some of the major concepts and principles on which environmental physics depends, we now consider how the transport of entities such as heat, mass, and momentum is determined by the state of the atmosphere and the corresponding state of the surface involved in the exchange, whether soil, vegetation, the coat of an animal, or the integument of an insect or seed.

General Transfer Equation

A simple general equation can be derived for transport within a gas by ―carriers,‖ which may be molecules or particles or eddies, capable of transporting units of a property P such as heat, water vapor, or a gas. Even when the carriers are moving randomly, net transport may occur in any direction provided that the concentration of P decreases with distance in that direction. The carrier can then ―unload‖ its excess of P at a point where the local value is less than at the starting point.

To evaluate the net flow of P in one dimension, consider a volume of gas with unit horizontal cross-section and a vertical height l assumed to be the mean distance for unloading a property of the carrier (Figure 3.1). Over the plane defining the base of the volume, P has a uniform value $P(0)$, and if the vertical gradient (change with height) of P is dP/dz, the value at height l will be $P(0)+l\ dP/dz$. Carriers which originate from a height l will therefore have a load corresponding to $P(0)+l\ dP/dz$, and if they move a distance l vertically downwards to the plane where the standard load corresponds to $P(0)$, they will be able to unload an excess of $l\ dP/dz$.

To find the rate of transport equivalent to this excess, assume that n carriers per unit volume move with a random *root mean square velocity v* so that the number moving toward one face of a cube at any instant is $nv/6$ per unit area. The downward flux of P (quantity per unit area and per unit time) is therefore given by $(nvl/6)dP/dz$. However, there is a corresponding upward flux of carriers reaching the same plane from below after setting off with a load given by $P(0)-l\ dP/dz$. Mathematically, the upward flow of a deficit is equivalent to the downward flow of an excess, so the net *downward* flux of P is

$$\mathbf{F} = (nvl/3)\,dP/dz.$$
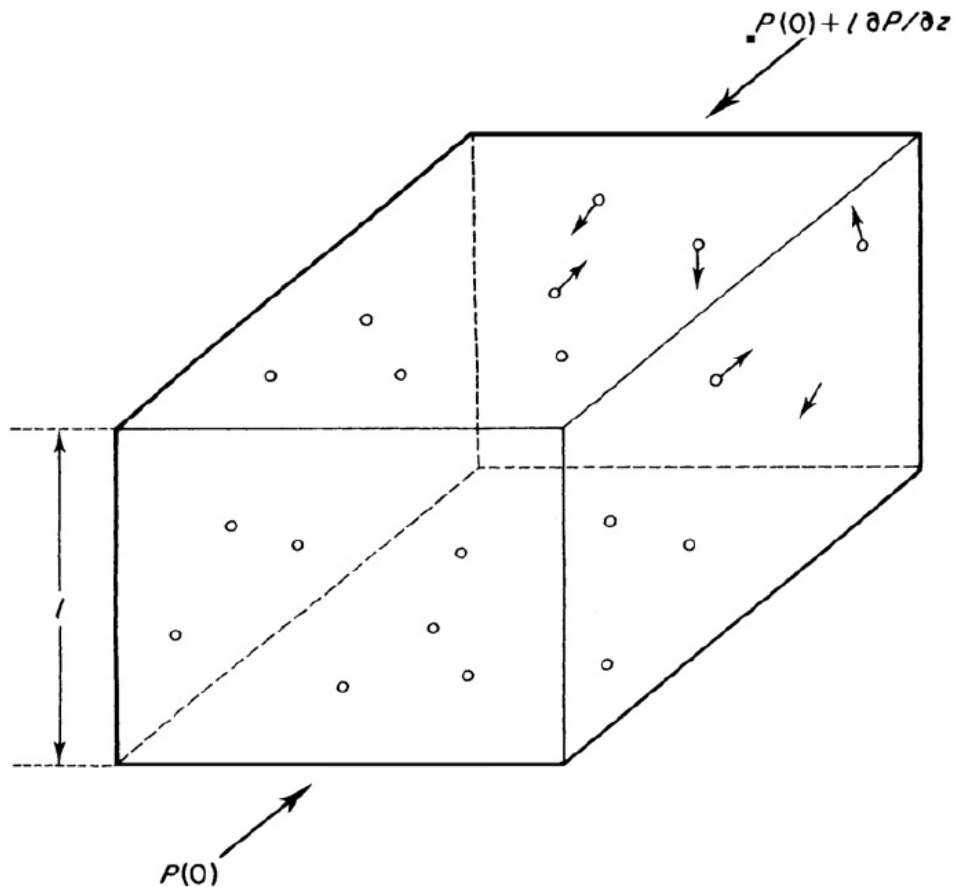
Figure 1 Volume of air with unit cross-section and height l containing n carriers per unit volume moving with random velocity v.

For the application of Eq. (3.1) to the transport of entities by molecular movement, the mean velocity in the z direction, w, is often related to the root mean square molecular velocity v by assuming that, at any instant, one-third of the molecules in the system are moving in the z direction so that $w = v/3$.

On the other hand, micrometeorologists studying transfer by turbulent eddies are concerned with a form of Eq. (3.1) in which P is replaced by the amount of an entity per unit mass of air (the *specific concentration*, q) rather than per unit volume (since the latter depends on temperature); the two quantities are related by $nP = \rho q$, where ρ is air density. The flux equation therefore becomes

$$\mathbf{F} = -\overline{\rho w l} \, (d\bar{q}/dz).$$

The minus sign is needed to indicate that the flux is downwards if q increases upwards; averaging bars are a reminder that both w and q fluctuate over a wide range

of time scales as a consequence of turbulence. In this context, the quantity l is known as the "mixing length" for turbulent transport.

It is also possible to write the instantaneous values of q and w as the sum of mean values $\bar{q}$ or $\bar{w}$ and corresponding deviations from the mean $q\_$ and $w\_$. The net flux across a plane then becomes

$$\overline{(\rho\bar{w} + \rho w')(\bar{q} + q')} = \overline{\rho w'q'},$$

Where $\bar{q}\_$ and $\bar{w}$

$\_$ are zero by definition and $\bar{w}$ is assumed to be zero near the ground when averaging is performed over a period long compared with the lifetime of the largest eddy (say 10 min). This relation provides the "eddy covariance" method of measuring Vertical fluxes discussed in Chapter 16.

Molecular Transfer Processes

According to Eq. (2.1), the mean square velocity of molecular motion in an ideal gas is $v2 = 3p/\rho$. Substituting $p = 105$ N m-2 and $\rho = 1.29$ kg m-3 for air at STP gives the root mean square velocity as $(v2)1/2 = 480$ m s-1, and the kinetic theory of gases may be used to show that the mean free path (the average distance a molecule travels between collisions) is 63 nm. Molecular motion in air is therefore extremely rapid over the whole range of temperatures found in nature, and collisions are frequent. This motion is responsible for a number of processes fundamental to micrometeorology: the transfer of momentum in moving air responsible for the phenomenon of viscosity; the transfer of heat by the process of conduction; and the transfer of mass by the diffusion of water vapor, carbon dioxide, and other gases. Because all three forms of transfer are a direct consequence of molecular agitation, they are described by similar relationships which will be considered for the simplest possible case of diffusion in one dimension only.

Momentum and Viscosity

When a stream of air flows over a solid surface, its velocity increases with distance from the surface. For a simple discussion of viscosity, the velocity gradient du/dz will be assumed linear as shown in Figure 3.2. (Amore realistic velocity profile will be

considered in Chapter 7.) Provided the air is isothermal, the velocity of molecular agitation will be the same at all distances from the surface but the horizontal component of bulk velocity in the x direction increases with vertical distance z. As a direct consequence of molecular agitation, there is a constant interchange of molecules between adjacent horizontal layers with a corresponding vertical exchange of horizontal momentum. The horizontal momentum of a molecule attributable to bulk motion of the gas as distinct from random motion is mu, so from Eq. (3.1) the rate of transfer of momentum, otherwise known as the *shearing stress*, can be written
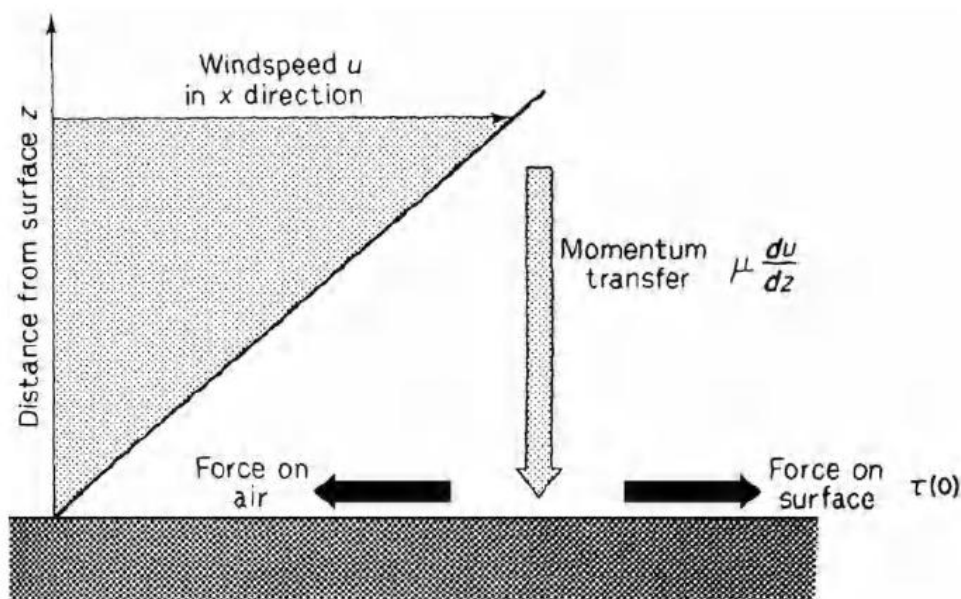
$$\tau = (nvl/3)\, d\,(mu)/dz = (vl/3)\, d\,(\rho u)/dz,$$

as the density of the gas is $\rho = mn$. This is formally identical to the empirical equation defining the *kinematic viscosity v* of a gas, viz.

$$\tau = vd(\rho u)/dz,$$

showing that v is a function of molecular velocity and mean free path. Where the change of ρ with distance is small, it is more convenient to write

$$\tau = \mu du/dz,$$

Figure 2 Transfer of momentum from moving air (moving left to right) to a stationary surface, showing related forces.

Where $\mu = \bar{\rho}\,v$ is the coefficient of *dynamic viscosity* and $\bar{\rho}$ is a mean density. By convention, the flux of momentum is taken as positive when it is directed *toward* a surface and it therefore has the same sign as the velocity gradient (see Figure 3.2). The momentum transferred layer by layer through the gas is finally absorbed by the surface which therefore experiences frictional force acting in the direction of the flow. The reaction to this force required by Newton's Third Law is the frictional drag exerted on the gas by the surface in a direction opposite to the flow.

Heat and Thermal Conductivity

The conduction of heat in still air is analogous to the transfer of momentum. In Figure 3.3, a layer of warm air makes contact with a cooler surface. The velocity of molecules therefore increases with distance from the surface and the exchange of molecules between adjacent layers of air is responsible for a net transfer of molecular energy and hence of heat. The rate of transfer of heat is proportional to the gradient of heat content per unit volume of the air and may therefore be written

$$C = -\kappa d(\rho c_{p} T)/dz,$$

where κ, the *thermal diffusivity* of air, has the same dimensions ($L^2\,T^{-1}$) as the kinematic viscosity and ρc_p is the heat content per unit volume of air. As in the treatment of momentum, it is convenient to assume that ρ has a constant value of $\bar{\rho}$ over the distance considered and to define a *thermal conductivity* as $k = \bar{\rho} c_p \kappa$ so that

$$C = -k\, dT/dz$$

Identical to the equation for the conduction of heat in solids.
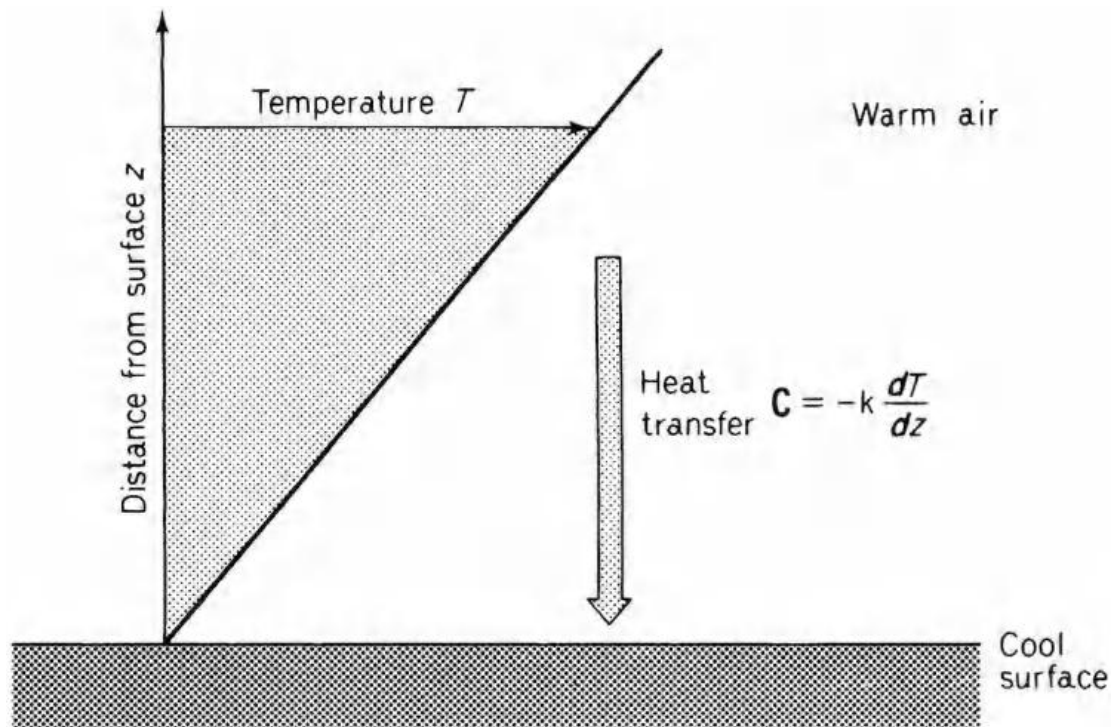
Figure 3 Transfer of heat from still, warm air to a cool surface.

In contrast to the convention for momentum, **C** is conventionally taken as positive when the flux of heat is *away* from the surface in which case dT/dz is negative. The equation therefore contains a minus sign.

*Mass Transfer and Diffusivity*

In the presence of a gradient of gas concentration, molecular agitation is responsible for a transfer of mass, generally referred to as "diffusion" although this word can also be applied to momentum and heat. In Figure 3.4, a layer of still air containing water vapor makes contact with a hygroscopic surface where water is absorbed. The number of molecules of vapor per unit volume increases with distance from the surface and the exchange of molecules between adjacent layers produces a net movement toward the surface. The transfer of molecules expressed as a mass flux per unit area *(E)* is proportional to the gradient of concentration and the transport equation analogous to Eqs. (3.6) and (3.8) is

$$\mathbf{E} = -D\,d\chi/dz = -Dd(\rho q)/dz = -\bar{\rho}D\,dq/dz,$$

where $\overline{\rho}$ is an appropriate mean density, D (dimensions L2 T−1) is the molecular diffusion coefficient forwater vapor, and q is the specific humidity. The sign convention in this equation is the same as for heat.

Diffusion Coefficients

Because the same process of molecular agitation is responsible for all three types of transfer, the diffusion coefficients for momentum, heat, water vapor, and other gases
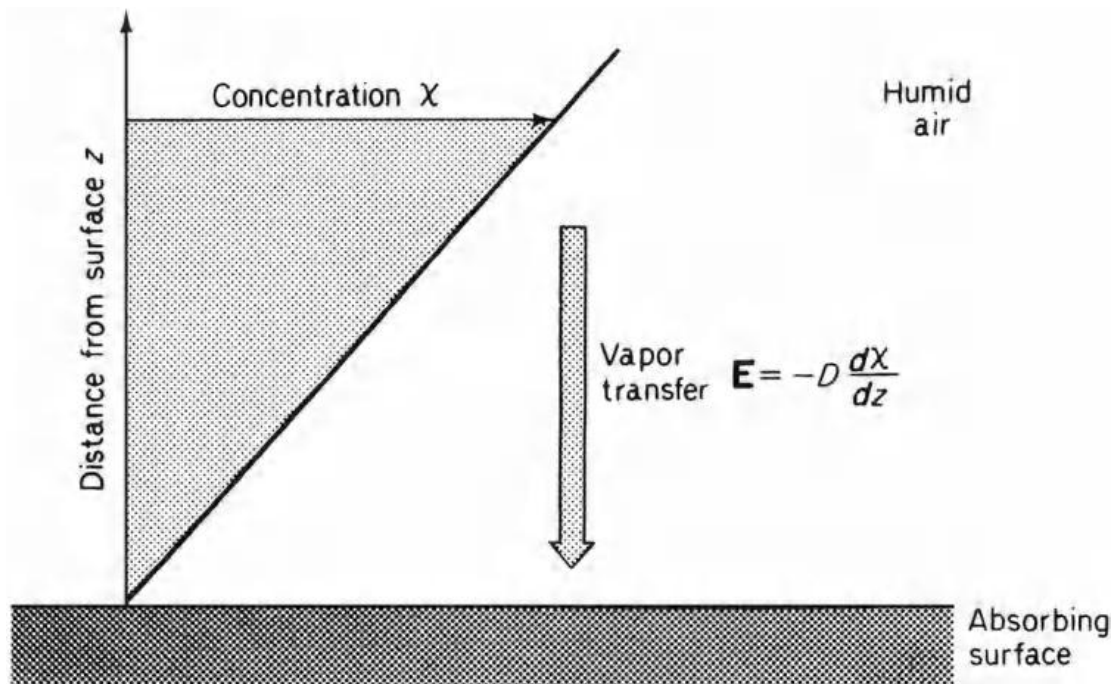
Figure 4 Transfer of vapor from humid air to an absorbing surface.

are similar in size and in their dependence on temperature. Values of the coefficients at different temperatures calculated from the Chapman-Eskog kinetic theory of gases agree well with measurements and are given in the Appendix, Table A.3. The temperature and pressure dependence of the diffusion coefficients is usually expressed by a power law, e.g.

$$D(T)/D(0) = \{T/T(0)\}^n \{P(0)/P\},$$

where $D(0)$ is the coefficient at base temperature and pressure $T(0)$ (K) and $P(0)$ respectively, and n is an index between 1.5 and 2.0. Within the limited range of temperatures relevant to environmental physics, say −10 to 50 ∘C, a simple temperature coefficient of 0.007 is accurate enough for practical purposes, i.e.

$$D(T)/D(0) = \kappa(T)/\kappa(0) = v(T)/v(0) = (1 + 0.007T),$$

where T is the temperature in $\circ$C and the coefficients in units of m2 s-1 are

$$v(0) = 13.3 \times 10^{-6} \text{ (momentum)},$$
$$\kappa(0) = 18.9 \times 10^{-6} \text{ (heat)},$$
$$D(0) = 21.2 \times 10^{-6} \text{ (water vapor)}$$
$$= 12.9 \times 10^{-6} \text{ (carbon dioxide)}.$$

Graham's Law states that the diffusion coefficients of gases are inversely proportional to the square roots of their densities, i.e. $D \propto$ *(M)* -0.5 since density is proportional to molecular weight. Consequently, the diffusion coefficient Dx for an unknown gas of molecular weight Mx can be estimated from values for a known gas (Dy, My) using the relation $Dx = Dy(My/Mx)0.5$.

1 Resistances to Transfer

Equations (3.5)–(3.7) have the same form flux = diffusion coefficient $\times$ gradient, which is a general statement of Fick's Law of Diffusion. This law can be applied to problems in which diffusion is a one-, two-, or three-dimensional process but only one dimensional cases will be considered here. Because the gradient of a quantity at a point is often difficult to estimate accurately, Fick's law is generally applied in an integrated form. The integration is very straightforward in cases where the (one-dimensional) flux can be treated as constant in the direction specified by the coordinate z, e.g. at right angles to a surface. Then the integration of (3.9) for example gives

$$\mathbf{E} = -\frac{\int_{z_1}^{z_2} d(\rho q)}{\int_{z_1}^{z_2} dz/D} = \frac{\rho q(z_1) - \rho q(z_2)}{\int_{z_1}^{z_2} dz/D},$$

where $\rho q(z1)$ and $\rho q(z2)$ are concentrations of water vapor at distances $z1$ and $z2$ from a surface absorbing or releasing water vapor at a rate **E**. Usually $\rho q(z1)$ is taken as the concentration at the surface so that $z1 = 0$. Equation (3.11) and similar equations derived by integrating Eqs. (3.6) and (3.8) are analogous to Ohm's Law in electrical circuits, i.e. current through resistance = potential difference across resistance. Equivalent expressions for diffusion can be written as:

rate of transfer of entity = potential difference resistance

$$\text{rate of momentum transfer } \tau = \rho u \Big/ \int dz/v,$$

$$\text{rate of heat transfer } \mathbf{C} = -\rho c_\mathrm{p} T \Big/ \int dz/\kappa,$$

$$\text{rate of mass transfer } \mathbf{E} = -\rho q \Big/ \int dz/D.$$

The definition of *resistance r* to mass transfer is therefore

$$r = \int dz/D$$

and similar equations define resistances to heat and momentum transfer. Diffusion coefficients have dimensions of (length) 2 × (time) so the corresponding resistances have dimensions of (time)/(length) or 1/(velocity). In a system where rates of diffusion are governed purely by molecular processes, the coefficients can usually be assumed independent of z so that $\_z2z1dz/D$, for example, becomes simply $(z2-z1)/D$ or (diffusion path length)/(diffusion coefficient).

Example 1. What is the resistance to water vapor diffusion by molecular agitation for a path length of 1 mm of air at 20 ∘C and 101.3 kPa?

Solution: The molecular diffusion coefficient of water vapor in air for the specified temperature and pressure is given in Appendix A.3, and is 24.9 × 10−6 m2 s−1.

Consequently the resistance for a pathlength of 1 mm (1×10^{-3} m) is $1 \times 10^{-3}/24.9 \times 10^{-6} = 40$ s m^{-1}.

It is often convenient to treat the process of diffusion in laminar boundary layers (layers where transfer is only by molecular motion) in terms of resistances, and in the remainder of this book the following symbols are used:

r_M resistance for momentum transfer at the surface of a body

r_H resistance for convective heat transfer

r_V resistance for water vapor transfer

r_C resistance for CO_2 transfer

The concept of resistance is not limited to molecular diffusion but is applicable to any system in which fluxes are uniquely related to gradients. In the atmosphere, where turbulence is the dominant mechanism of diffusion, diffusion coefficients are several orders of magnitude larger than the corresponding molecular values and increase with height above the ground (Chapter 16). Diffusion resistances for momentum, heat, water vapor and carbon dioxide in the atmosphere will be distinguished by the symbols r_{aM}, r_{aH}, r_{aV}, and r_{aC};

In studies of the deposition of radioactive material and pollutant gases from the atmosphere to the surface, the rate of transfer is sometimes expressed as a *deposition velocity*, which is the reciprocal of a diffusion resistance. In this case, the surface concentration is often assumed to be zero and the deposition velocity is found by dividing the rate of deposition of the material by its concentration at an arbitrary height.

Plant physiologists also frequently use the reciprocal of resistance (in this context termed *conductance*) to describe transfer between leaves and the atmosphere, arguing that the direct proportionality between *flux* and *conductance* is a more intuitive concept than the inverse relationship between flux and resistance. In this book we generally prefer the resistance formulation because of its familiarity to physicists, particularly when combinations of resistances in parallel and series must be calculated.

1 Alternative Units for Resistance and Conductance

Units of sm^{-1} for resistance andms^{-1} for conductance are the result of expressing mass fluxes as mass flux density (e.g. kg m^{-2} s^{-1}) and driving potentials as concentrations (e.g. kg m^{-3}). The forms of the equations for momentum, heat, and

mass transfer (3.12) ensure that resistance units for these variables are also s m−1. A criticism of this convention is that, when resistance is defined as (diffusion path length)/(diffusion coefficient), r is proportional to pressure P and inversely approximately proportional to T^2 (see Eq. (3.10)). Thus, for example, analyzing the effects of altitude on fluxes can be confusing. Alternative definitions of resistance units, less sensitive to temperature and pressure, are sometimes used, particularly by plant physiologists, as follows.

Since biochemical reactions concern numbers of molecules reacting, rather than the mass of substances, it is convenient to express fluxes in *mole flux density*, J (mol m−2 s−1). Similarly, amount of the substance can be expressed as the *mole fraction x*, i.e. the number of moles of the substance as a fraction of the total number of moles in the mixture (mol mol−1). Using the Gas Laws, it is readily shown that mass concentration χ (kg m−3), or its equivalent ρq, is related to x by

$$\chi = \rho q = xP/RT,$$

so Eq. (3.9) may be written

$$J = \frac{x(z_1) - x(z_2)}{\frac{RT}{P} \int dz/D}$$

or, since $x = p/P$, where p is the partial pressure,

$$J = \frac{p(z_1) - p(z_2)}{RT \int dz/D}.$$

The molar resistance r_m (m^2 s mol^{-1}) is defined as

$$r_m = \frac{RT}{P} \int \frac{dz}{D} = \frac{RT}{P} r$$

demonstrating that r_m is independent of pressure and less dependent on temperature than r . pointed out that it is important to use partial pressure or mole fraction to describe potentials that drive diffusion when systems are not isothermal. At 20 ∘C and 101.3 k Pa, the approximate conversion between resistance units is r m(m2 s mol−1) = 0.024r (s m−1).

Diffusion of Particles (Brownian Motion)

The random motion of particles suspended in a fluid or gas was first described by the English botanist Brown in 1827, but it was nearly 80 years before Einstein used the kinetic theory of gases to show that the motion was the result of multiple collisions with the surrounding molecules. He found that the mean square displacement x^2 of a particle in time t is given by

$$x^2 = 2Dt, \quad (3.16)$$

where D is a diffusion coefficient (dimensions $L^2\,T^{-1}$) for the particle, analogous to the coefficient for gas molecules. The quantity D depends on the intensity of molecular bombardment (a function of absolute temperature), and on the viscosity of the fluid, as follows.

Suppose that particles, each with mass m (kg), are dispersed in a container where they neither stick to the walls nor coagulate. The Boltzmann statistical description of concentration, derived from kinetic theory, requires that, as a consequence of the earth's gravitational field, the particle concentration n should decrease exponentially with height z(m) according to the relation

$n = n(0) \exp(-mgz/kT), \quad (3.17)$

where

$n = n(0)$ at $z = 0$,

g = gravitational acceleration$(m\,s^{-2})$,

T = absolute temperature (K),

k = Boltzmann's constant (J K^{-1}).

Across a horizontal area at height z within the container, the flux of particles upwards by diffusion (cf. diffusion of gases) is:

$$\mathbf{F}_1 = -D\frac{dn}{dz} = n\frac{Dmg}{kT}$$

from Eq. (3.17). Because all particles tend to move downwards in response to gravity, there must be a downward flux through the area of

F2 = nVs,

where Vs is the ―sedimentation velocity"

Since the system is in equilibrium, **F1** = **F2** and so

$D = kT V$s$/mg$. (3.19)

For spherical particles, radius r, obeying Stokes' Law, the downward force mg due to gravity is balanced by a drag force $6\pi\rho$gvrVs, where ρg is the gas density and v is the kinematic viscosity (see Chapter 9). Consequently

$D = kT /6\pi\rho$gvr . (3.20)

Thus D depends inversely on particle radius (see Appendix, Table A.6); its dependence on temperature is dominated by the dependence of the kinematic viscosity v on temperature. Equations (3.16) and (3.17) show that the root mean square displacement of a particle by Brownian motion is proportional to T 0.5 and to r−0.5. Surprisingly, $\overline{x^2}$ does not depend on the mass of the particle, an inference confirmed by experiment.

Problems

1. Calculate the resistance (in s m−1) for carbon dioxide diffusion in air over a path length of 1 mm, assuming air temperature is 20 ∘C and atmospheric pressure is 101 kPa. Recalculate the resistance assuming that atmospheric pressure decreased to 70 kPa (keeping temperature constant). Repeat the two calculations using molar units.

2. Use the data in the Appendix Table A.6 to investigate how the diffusion coefficient of particles depends on temperature.

The Origin and Nature of Radiation

Electromagnetic radiation is a form of energy derived from oscillating magnetic and electrostatic fields and is capable of transmission through empty space where its velocity is c = 3.0 × 108 m s−1. The frequency of oscillation v is related to the wavelength λ by the standard wave equation $c = \lambda v$ and the wave number $1/\lambda = v/c$ is sometimes used as an index of frequency.

The ability to emit and absorb radiation is an intrinsic property of solids, liquids, and gases and is always associated with changes in the energy state of atoms and

molecules. Changes in the energy state of atomic electrons are associated with line spectra confined to a specific frequency or set of frequencies. In molecules, the energy of radiation is derived from the vibration and rotation of individual atoms within the molecular structure. The principle of energy conservation is fundamental to the material origin of radiation. The amount of radiant energy emitted by an individual atom or molecule is equal to the decrease in the potential energy of its constituents.

Absorption and Emission of Radiation

All molecules possess a certain amount of ―internal" energy (i.e. not associated with their motion in the atmosphere).Most of the energy is associated with electrons orbiting around the nucleus, but part is related to vibration of atoms in the molecular structure and to rotation of the molecule. Quantum physics predicts that only certain electron orbits, vibration frequencies, and rotation rates are allowed for a particular molecule, and each combination of orbits, vibrations, and rotations corresponds to a particular amount of energy associated with the three features. Molecules may make a transition to a higher or lower energy level by absorbing or emitting electromagnetic radiation respectively.

Quantum theory allows only certain discrete changes in energy levels, which are the same whether the energy is being absorbed or emitted. Since the energy associated with a photon is related to its wavelength by $E = hc/\lambda$, where h is Planck's constant, it follows that molecules can interact only with certain wavelengths of radiation. Thus the variation of absorption and emission of molecules with wavelength takes the form of a *line spectrum*, consisting of a finite number of wavelengths where interaction is allowed, interspaced by gaps where there is no interaction.

Most absorption lines associated with orbital changes are in the X-ray, UV, and visible spectrum. Vibrational changes are associated with absorption at infrared wavelengths, and rotational changes correspond to lines at even longer, microwave wave lengths. Molecules such as CO_2, H_2O, and O_3 have structures that allow vibration rotational transitions simultaneously, and these correspond to clusters of very closely spaced lines in the infrared region. Molecules such as O_2 do not interact this way, so have only small numbers of absorption lines.

When large numbers of molecules are present in a gas, the width of their absorption and emission lines is greatly enhanced by broadening associated with random

molecular motions (*Doppler broadening*—depending on the square root of absolute temperature) and with interactions during collisions (*collision broadening*—depending on the frequency of collisions, which is proportional to gas pressure). Collision broadening is most important for atmospheric molecules below about 30 km and results in overlapping of lines in the clusters associated with vibration-rotational transitions in CO2 and H2O, creating *absorption bands* in the infrared for these gases. Since pressure decreases with increasing height, the absorptivity and emissivity of a gas distributed in the lower atmosphere with a constant mixing ratio changes with height, making calculations of radiative transfer complex.

Full or Black Body Radiation

Relations between radiation absorbed and emitted by matter were examined by Kirchhoff. He defined the absorptivity of a surface $\alpha(\lambda)$ as the fraction of incident radiation absorbed at a specific wavelength λ. The emissivity $\varepsilon(\lambda)$ was defined as the ratio of the actual radiation emitted at thewavelength λ to a hypothetical amount of radiant flux **B***(λ)*. By considering the thermal equilibrium of an object inside an enclosure at a uniform temperature, he showed that $\alpha(\lambda)$ is always equal to $\varepsilon(\lambda)$. For an object completely absorbing radiation at wavelength λ, $\alpha(\lambda) = 1$, $\varepsilon(\lambda) = 1$, and the emitted radiation is **B***(λ)*. In the special case of an object with $\varepsilon = 1$ at *all* wavelengths, the spectrum of emitted radiation is known as the ―full‖ or *black body spectrum*. Within the range of temperatures prevailing at the earth's surface, nearly all the radiation emitted by full radiators is confined to the waveband 3–100 μm, and most natural objects—soil, vegetation, water—behave radiatively almost like full radiators in this restricted region of the spectrum (but not in the visible spectrum). Even fresh snow, one of the whitest surfaces in nature, emits radiation like a black body between 3 and 100 μm. The statement ―snow behaves like a black body‖ refers therefore to the radiation *emitted* by a snow surface and not to solar radiation *reflected* by snow. The semantic confusion inherent in the term ―black body‖ can be avoided by referring to ―*full radiation*‖ and to a ―*full radiator.*‖

After Kirchhoff's work was published in 1859, the emission of radiation by matter was investigated by a number of experimental and theoretical physicists. By combining a spectrometer with a sensitive thermopile, it was established that the spectral distribution of radiation from a full radiator resembles the curve in Figure 4.1 in which the chosen temperatures of 6000 and 300 K correspond approximately to the

mean full radiation temperatures of the sun and the earth's surface. A theoretical explanation of
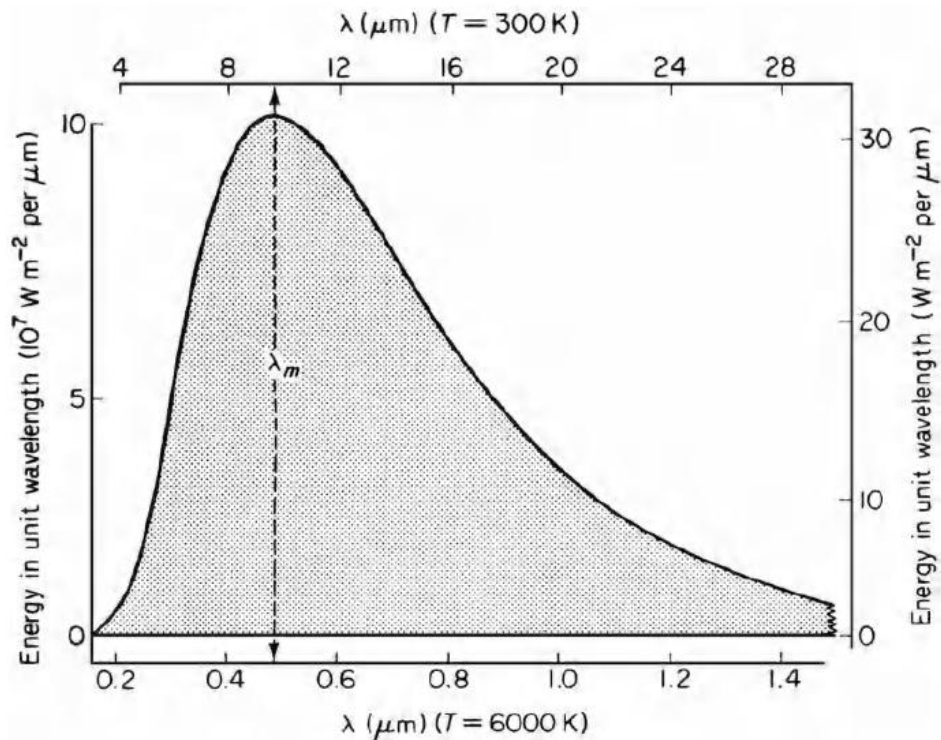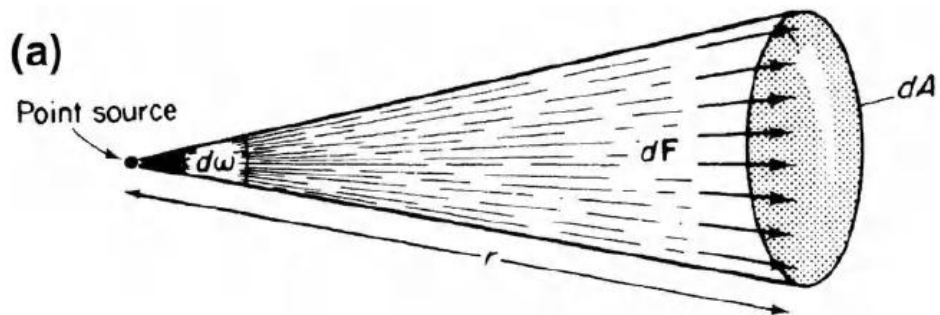

Figure 1 Spectral distribution of radiant energy from a full radiator at a temperature of (a) 6000 K, left-hand vertical and lower horizontal axis and (b) 300 K, right-hand vertical and upper horizontal axis. Note that the scales on the left and right vertical axes differ by more than six orders of magnitude. About 10% of the energy is emitted at wavelengths longer than those shown in the diagram. If this tail were included, the total area under the curve would be proportional to $\zeta T 4$ (Wm−2). λm is the wavelength at which the energy per unit wavelength is maximal. The distribution eluded physicists until Plank's quantum hypothesis emerged (Section 4.1.5).
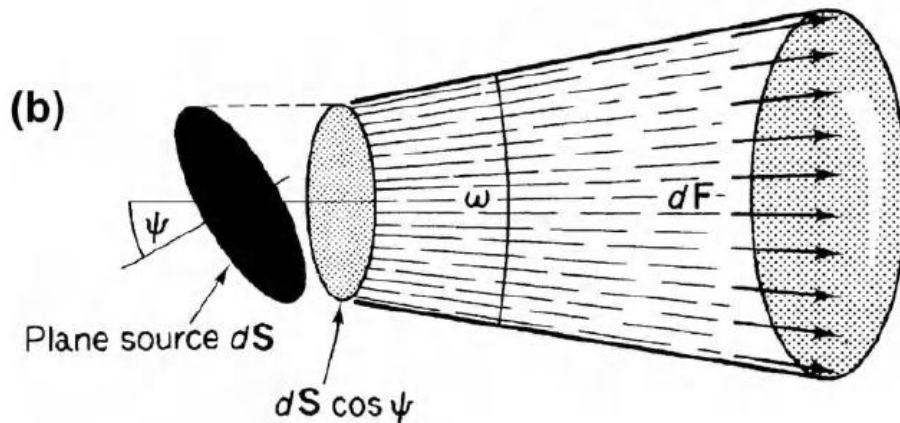

Cosine Law for Emission and Absorption

The concept of radiance is linked to an important law describing the spatial distribution of radiation emitted by a full radiator which has a uniform surface temperature T. This temperature determines the total flux of energy emitted by the surface $(\zeta T 4)$ and can be estimated by measuring the radiance of the surface with a radiometer. As the surface of a full radiator must appear to have the same temperature whatever angle ψ it is viewed from, the intensity of radiation emitted from a point on the surface and the radiance of an element of surface must both be independent of ψ.

On the other hand, the flux per unit solid angle divided by the *true* area of the surface must be proportional to cosψ. Figure 3 makes this point diagrammatically. A radiometer R mounted vertically above an extended horizontal surface *XY* "sees" an area *dA* and measures a flux which is proportional to *dA*. When the surface is tilted through an angle ψ, the radiometer now sees a larger surface *dA*/ cosψ, but provided the temperature of the surface stays the same, its radiance will be constant and the flux recorded by the radiometer will also be constant. It follows that the flux emitted per unit area (the emittance of the surface) at an angle ψ must be proportional to cosψ so that the product of emittance

(a)

Point source

$dω$

dF

dA

r

Solid angle $dω = dA/r^2$
Intensity $I = dF/dω$

(b)

ψ

Plane source dS

$dS \cos ψ$

$ω$

dF

Intensity $dI = dF/ω$
Radiance $= (dF/ω) \div dS \cos ψ$
$= dI/(dS \cos ψ)$

Figure 2 (a) Geometry of radiation emitted by a point source. (b) Geometry of radiation emitted by a surface element. In both diagrams a portion of a spherical surface receives radiation at normal incidence, but when the distance between the source and the receiving surface is large, it can be treated as a plane.

($\propto \cos\psi$) and the area emitting to the instrument ($\propto 1/\cos\psi$) stay the same for all values of ψ. This argument is the basis of *Lambert's Cosine Law* which states that when radiation is emitted by a full radiator at an angle ψ to the normal, the flux per unit solid angle emitted by unit surface is proportional to $\cos\psi$. As a corollary to Lambert's Law, it can be shown by simple geometry that when a full radiator is exposed to a beam of radiant energy at an angle ψ to the normal, the flux density of the absorbed radiation is proportional to $\cos\psi$. In remote sensing it is often necessary to specify the directions of both incident and reflected radiation, and reflectivity is then described as ‒bi-directional."
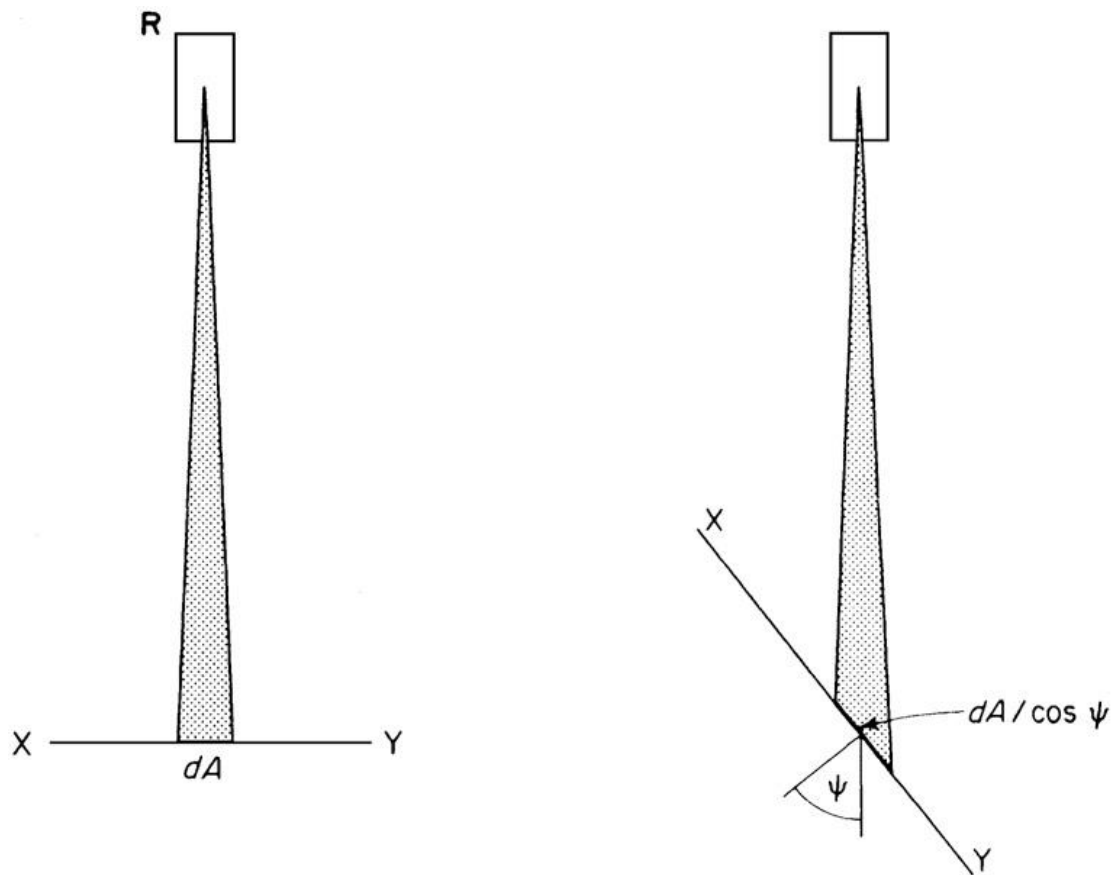
Figure 3 The amount of radiation received by a radiometer from the surface *XY* is independent of the angle of emission, but the flux emitted per unit area is proportional to cosψ.

Reflection

The reflectivity of a surface $\rho(\lambda)$ is defined as the ratio of the incident flux to the reflected flux at the same wavelength. Two extreme types of behavior can be distinguished. For surfaces exhibiting specular or mirror-like reflection, a beam of radiation incident at an angle ψ to the normal is reflected at the complementary angle $(-\psi)$. On the other hand, the radiation scattered by a perfectly diffuse reflector (also called a *Lambertian* surface) is distributed in all directions according to the Cosine Law, i.e. the intensity of the scattered radiation is independent of the angle of reflection but the flux scattered from a specific area is proportional to cosψ. The nature of reflection from the surface of an object depends in a complex way on its electrical properties and on the structure of the surface. In general, specular reflection assumes increasing importance as the angle of incidence increases, and surfaces

acting as specular reflectors absorb less radiation than diffuse reflectors made of the same material.

Most natural surfaces act as diffuse reflectors when ψ is less than 60° or 70°, but as ψ approaches 90°, a condition known as *grazing incidence*, the reflection from open water, waxy leaves, and other smooth surfaces becomes dominantly specular and there is a corresponding increase in reflectivity. The effect is often visible at sunrise and sunset over an extensive water surface, or a lawn, or a field of barley in ear.

When surfaces are observed by techniques of remote sensing, the direction of the radiation received by the radiometer is significant, and several additional definitions are necessary:

Bi-directional reflectance (sr−1) is the ratio of the radiation *reflected* in a specific direction of view to the radiation *incident* in that direction. The *Bi-directional reflectance factor* of a surface (BRF) is the ratio of the reflected radiance from a specific view direction to the radiance that would be observed from a perfectly diffuse surface at the same location. Most examples in this book deal with a plane surface below a uniform hemispherical source of radiation (e.g. an overcast sky). The fraction of incident radiation reflected from such a surface is sometimes referred to as the *bi-hemispherical reflectance* or simply the *reflection coefficient*. The reflection coefficient for solar radiation is commonly known as the *albedo*.

Radiance and Irradiance

When a plane surface is surrounded by a uniform source of radiant energy, a simple relation exists betweenthe irradiance of the surface (the flux incident per unit area) and the radiance of the source. Figure 4.4 displays a surface of unit area surrounded by a radiating hemispherical shell so large that the surface can be treated as a point at the center of the hemisphere. The shaded area dS is a small element of radiating surface and the radiation reaching the center of the hemisphere from dS makes an angle β with the normal to the plane. As the projection of unit area in the direction of the radiation is $1 \times \cos \beta$, the solid angle which the area subtends at dS is $\omega = \cos \beta / r$
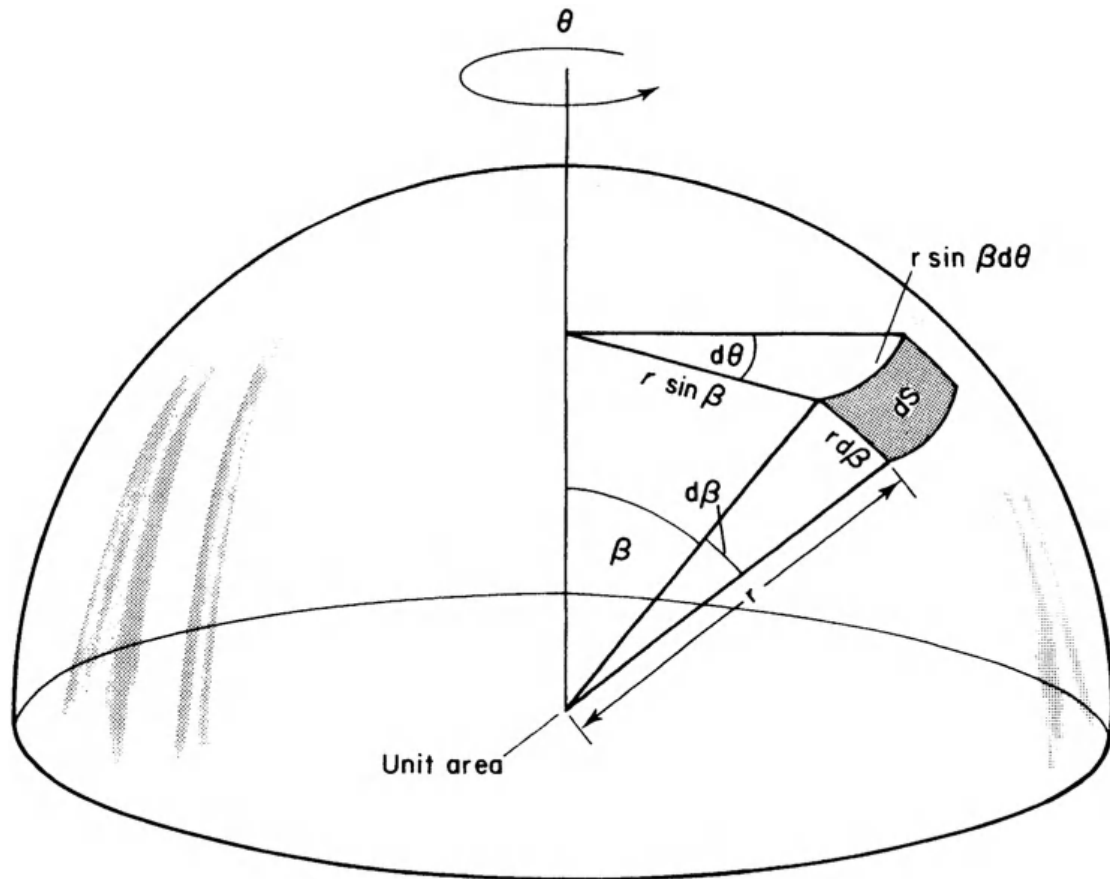
Figure 4 Method for calculating irradiance at the center of an equatorial plane from a surface element dS at angle β to vertical axis.

If the element dS has a radiance **N**, the flux emitted by dS in the direction of the plane must be $\mathbf{N} \times dS \times \omega = \mathbf{N}dS \cos \beta/r\ 2$. To find the total irradiance of the plane, this quantity must be integrated over the whole hemisphere, but if the radiance is uniform, conventional calculus can be avoided by noting that $dS \cos \beta$ is the area dS projected on the equatorial plane. It follows that _ $dS \cos \beta$ is the area of the whole plane or πr 2, so that the total irradiance at the center of the plane becomes

$$(\mathbf{N}/r^2) \int \cos \beta \, dS = \pi \mathbf{N}.$$

The irradiance expressed in Wm−2 is therefore found by multiplying the radiance in Wm−2 sr−1 by the solid angle π. A more rigorous treatment is needed if the radiance depends on the position of dS with respect to the surface receiving radiation. It is necessary to treat dS as a rectangle whose sides are $rd\beta$ and $r \sin \beta d\theta$ where θ is an

azimuth angle with respect to the axis of the hemisphere, radius r. Given that $dS = r2 \sin \beta d\beta d\theta$, the integral becomes

$$\int_{\theta=0}^{2\pi} \int_{\beta=0}^{\pi/2} N(\beta, \theta) \left(\frac{\cos \beta}{r^2} \right) r^2 \sin \beta \, d\beta \, d\theta.$$

If N is independent of azimuth (i.e. only a function of β), Eq. (4.9) simplifies to

$$= 2\pi \int_{\beta=0}^{\pi/2} N(\beta) \sin \beta \cos \beta \, d\beta$$

$$= \pi \int_{\beta=0}^{\pi/2} N(\beta) \sin 2\beta \, d\beta.$$

Attenuation of a Parallel Beam

When a beam of radiation consisting of parallel rays of radiation passes through a gas or liquid, quanta encounter molecules of the medium or particles in suspension. After interacting with the molecule or particle, a quantum may suffer one of two fates: it may be absorbed, thereby increasing the energy of the absorbing molecule or particle; or it may be scattered, i.e. diverted from its previous course either forwards (within 90° of the beam) or backwards in a process akin to reflection from a solid. After transmission through the medium, the beam is said to be ―attenuated‖ by losses caused by absorption and scattering.

Beer's Law, frequently invoked in environmental physics, describes attenuation in a very simple system where radiation of a single wavelength is absorbed but not scattered when it passes through a homogeneous medium. Suppose that at some distance x into the medium the flux density of radiation is _(x) (Figure 4.5).

Absorption in a thin layer dx, assumed proportional to dx and to _(x), may be written

$$d\_ = -k\_(x)dx,$$
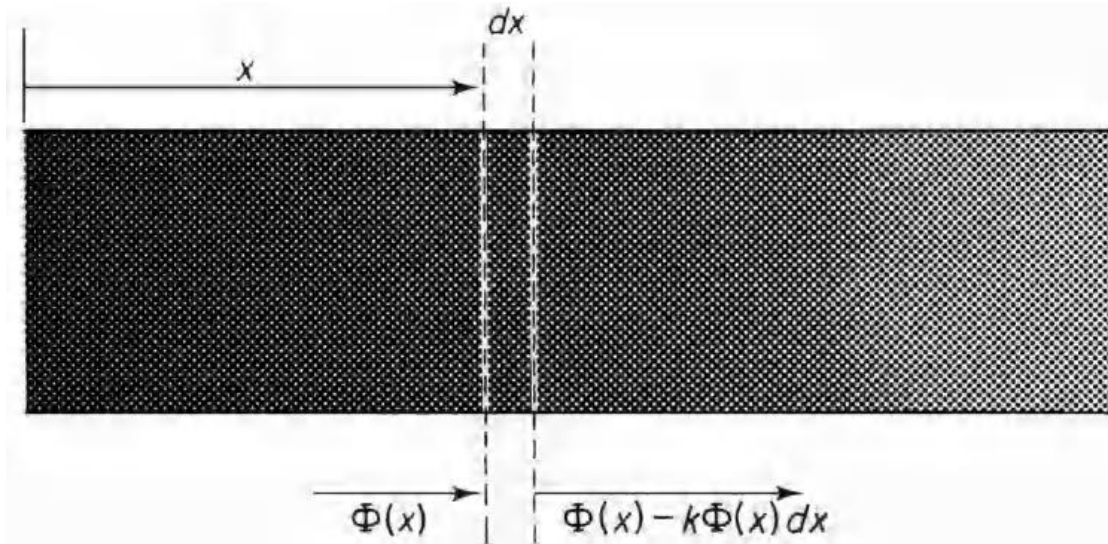
Figure 5 The absorption of a parallel beam of monochromatic radiation in a homogeneous medium with an absorption coefficient k. $\_(0)$ is the incident flux, $\_(x)$ is the flux at depth x, and the flux absorbed in a thin layer dx is $k\_(x)dx$.

where the constant of proportionality k, described as an "attenuation coefficient," is the probability of a quantum being intercepted within the small distance dx. Integration gives

$\_(x) = \_(0) \exp(-kx)$, (4.12)

where $\_(0)$ is the flux density at $x = 0$.

Beer's Law can also be applied to radiation in a waveband over which k is constant; or to a system in which the concentration of scattering centers is so small that a quantum is unlikely to interact more than once ("single scattering"). The treatment of *multiple scattering* is much more complex for two main reasons: (a) radiation in a beam scattered backwards must be considered as well as the forward beam; (b) if k depends on beam direction, the angular distribution of scattering must be taken into account. For the simplest case where k is independent of beam direction, equations of a type developed by Kubelka and Munk are valid. They allow the attenuation coefficient to be expressed as a function of a reflection coefficient ρ which is the probability of an interacting quantum being reflected backwards and η which is the probability of forward scattering, implying that the probability of absorption is

$\alpha = 1 - \rho - \eta$.

In a system with multiple scattering, it is necessary to distinguish two streams of radiation. One moves *into* the medium, and at a distance x from the boundary has a flux density $\_+(x)$.

The other, generated by scattering, moves *out* of the medium with a flux density $\Phi_-(x)$. The inward flux is depleted by absorption and reflection but is augmented by reflection of a fraction of the outward stream. The *net* loss of inward flux at a depth x and in a distance dx is therefore

$$d\Phi_+(x) = (-(\alpha + \rho)\Phi_+(x) + \rho\Phi_-(x))dx, \quad (4.13)$$

where $(\alpha + \rho)$ is a probability of interception.

The outward stream is also weakened by absorption and reflection but is augmented by reflection of the inward stream to give a net outward flux of

$$d\Phi_-(x) = -((\alpha + \rho)\Phi_-(x) - \rho\Phi_+(x))dx, \quad (4.14)$$

where the minus sign in front of the brackets is a reminder that the outward flux is moving in a negative direction with respect to the x axis.

For the special case of uniform scattering in all directions (isotropic scattering), $\rho = \eta = \alpha/2$. It may then be shown that the bulk reflection coefficient ρ_* is given by

$$\rho_* = (1 - \alpha^{0.5})/(1 + \alpha^{0.5}), \quad (4.15)$$

and the bulk attenuation coefficient k_* is given by

$$k_* = \alpha^{0.5}. \quad (4.16)$$

(These equations are not relevant to the limiting case $\alpha = 1$ when Beer's Law applies.) When the forward beam strikes a boundary before it is completely attenuated, a fraction ρb may be reflected. The fluxes of radiation in the medium, both forwards and backwards, can then be expressed as functions of $\rho b, \rho, \eta$ and of the concentration of the medium. Complex numerical methods must be deployed to obtain fluxes when condition

(b) is not satisfied, i.e. when k is a function of the direction of scattering examples of the application of Beer's Law to the atmosphere (where the assumption of single scattering is usually valid). application of the Kubelka-Munk equations is discussed with reference to crop canopies and animal coats.

Problems

1. Ultra-violet radiation in the waveband 280–320 nm incident at the top of the earth's atmosphere supplies about $20 Wm^{-2}$ of radiant energy at normal incidence. Assuming a mean wavelength of 300 nm, calculate the photon flux at normal incidence.

2. At what wavelength does the peak emission from an oxyacetylene welding torch burning at 3800 K occur?

Radiation Environment

Almost all the energy for physical and biological processes at the earth's surface comes from the sun and much of environmental physics is concerned with ways in which this energy is dispersed or stored in thermal, mechanical, or chemical form. considers the quantity and quality of solar (short-wave) radiation received at the ground and the exchange of terrestrial (long-wave) radiation between the ground and the atmosphere.

Solar Radiation

1 Solar Constant

At themean distance R of the earth from the sun, which is 1.50×108 km, the irradiance of a surface perpendicular to the solar beam and just outside the earth's atmosphere is known as the *Solar Constant*. The name is somewhat misleading because this quantity is known to change by small amounts over periods of weeks to years in response to changes within the sun, and the preferred term to describe the irradiance at mean earth-sun distance is the *Total Solar Irradiance*, TSI.

Increasingly precise determinations of the TSI have been made from mountain tops, balloons, rocket aircraft flying above the stratosphere and, since the late 1970s, from satellites. Satellite observations have clearly demonstrated that the annual mean TSI varies by about 1.6 W m−2 between the minimum and maximum of the 11-year cycle of solar activity (Figure 1) (Frohlich and Lean, 1998; Kopp and Lean, 2011). Although satellite radiometers are capable of great precision, their absolute accuracy is much poorer. Kopp and Lean (2011) used data from an improved satellite radiometer to conclude that the most probable absolute value of the TSI representative of solar minimum activity is 1361 ± 0.5 W m−2, about 5 W m−2 lower than the value recommended in about 2000. The downward revision is attributed to improved measurement accuracy, not a change in solar activity. Indirect proxies that vary with TSI (e.g. sunspot number) suggest that the total solar irradiance (Solar Constant) may have increased by about 0.3 W m−2 since 1750, thus making a minor contribution to global warming, but reliability of this estimate is poor (IPCC, 2007). The spectrum of radiation from the sun closely resembles that of a full (black body) radiator, and the temperature of the equivalent full radiator may be readily estimated from knowledge of the TSI as follows. Assuming that the sun radiates uniformly in all directions, the

earth intercepts only a small fraction of the radiated solar energy passing across the surface of an imaginary
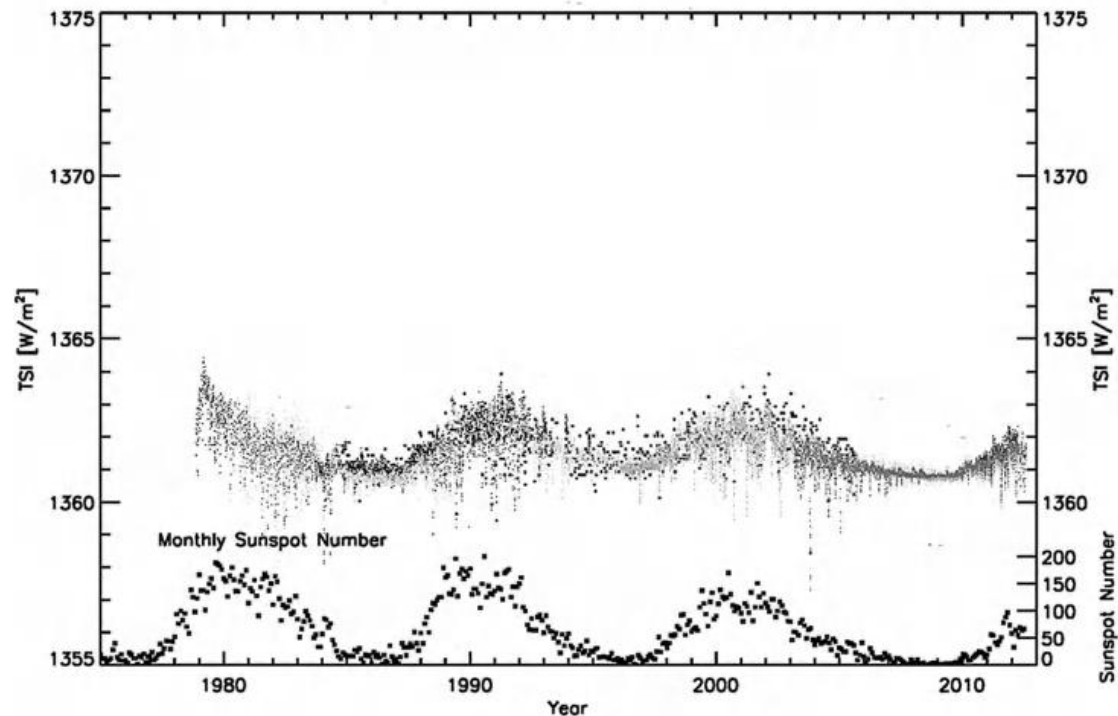
Figure 1 Composite record of total solar irradiance, TSI (the ―Solar Constant"), from 1975 to 2012 compiled from multiple satellite radiometric measurements adjusted to a standard reference scale. Also shown is the monthly mean sunspot number, illustrating the strong correlation with TSI. (data courtesy of Greg Kopp, NASA.)

sphere centered at the sun and with radius R, the earth's mean distance from the sun (149.6×109 m*)*. The total rate at which energy is emitted from the sun may therefore be calculated by multiplying the TSI by the surface area of the sphere, i.e.

$E = 4\pi R2 \times 1361 = 3.83 \times 1026$ W.

The radius of the sun is $r = 6.96 \times 108$ m. Hence, assuming the surface behaves like a full radiator, its effective temperature T is given by

$\zeta T4 = 3.83 \times 1026/(4\pi r 2)$, from which the (rounded) value of T is 5771 K.

2 Sun-Earth Geometry

Major features of radiation at the surface of the earth are determined by the earth's rotation about its own axis and by its elliptical orbit around the sun. The polar axis

about which the earth rotates is fixed in space (pointing at the Pole Star) at a mean angle of 66.5∘ to the plane of the earth's orbit (termed the *obliquity*) but with a small top-like wobble (the *precession* of the axis). The angle between the orbital plane and the earth's equatorial plane therefore oscillates between a maximum of 90–66.5 = 23.5∘ in midsummer and a minimum of −23.5∘ in midwinter with small deviations attributable to the wobble. This angle is known as the *solar declination (δ)* and its value for any date and year can be found from astronomical tables.

The shape of the earth's orbit (the *eccentricity*), obliquity, and precession each vary over millenia, with cycles ranging from about 100,000 to 23,000 years. The Russian astronomer Milutin Milankovitch proposed in the 1930s that these orbital variations were responsible for long-term cyclical changes in the earth's climate. Modern evidence from the analysis of layers of deep ocean sediments has confirmed that the *Milankovitch theory* explains part, but not all, of the variations in climate over the past few hundred thousand years.

Currently, the eccentricity of the earth's orbit is relatively small. The earth is about 3%closer to the sun in January than in July, so the irradiance at the top of the atmosphere is almost 7% larger in January (irradiance is proportional to the inverse square of the sun-earth radius). At any point on the earth's surface, the angle between the direction of the sun and a vertical axis depends on the latitude of the site, and on time t (hours), most conveniently referred to the time when the sun reaches its zenith. The hour angle θ (radians) of the sun is the fraction of 2π through which the earth has turned after local solar noon, i.e. $\theta = 2\pi t/24$. Since $2\pi \equiv 360\circ$, each hour corresponds to 15∘ rotation.

Three-dimensional geometry is needed to show that the *zenith angle ψ* of the sun at latitude ϕ is given by:

$\cos\psi = \sin\phi \sin\delta + \cos\phi \cos\delta \cos\theta$ (5.1)

and that the azimuth angle A of the sun with respect to south is given by:

$\sin A = -\cos\delta \sin\theta/\sin\psi.$ (5.2)

The minimum zenith angle of the sun ψn occurs at local solar noon and may be found by putting $\theta = 0$ in Eq. (5.1) to give

$\cos\psi$n $= \sin\phi \sin\delta + \cos\phi \cos\delta$

$= \cos(\phi - \delta)$

so

ψn $= \phi - \delta.$ (5.3)

To find the *daylength*, defined as the period for which the sun is above the horizon, the hour angle θ_s at sunset (i.e. the half-day length t) is first found by putting $\psi = \pi/2$ radians (90°) in Eq. (5.1), and rearranging to give:

$$\cos\theta_s = -\frac{\sin\varphi \, \sin\delta}{\cos\varphi \, \cos\delta} = -\tan\varphi \tan\delta,$$

$$\theta_s = 2\pi t/24 = \cos^{-1}(-\tan\varphi \tan\delta),$$

from which the daylength $2t$ in hours is

$$2t = (24/\pi)\theta_s = (24/\pi)\cos^{-1}(-\tan\varphi \tan\delta).$$

Some developmental processes in plants and activity in animals occur at the very weak levels of radiation received during twilight before sunrise and after sunset. The biological length of a day may therefore exceed the daylength given by Eq. (5.6) to an extent which can be estimated from the time of *civil twilight* (sun dropping to 6° below horizon with a correction for refraction, i.e. $\psi = 96$° or 1.68 radians) or *astronomical twilight* (down to 18° below horizon, $\psi = 108$° or 1.89 radians). The beginning of civil and astronomical twilight can be calculated from Eq. (5.1) by substituting these values of ψ. At the equator, the interval between civil twilight and sunrise is close to 22 min throughout the year but at latitude 50° it ranges from 45 min at midsummer to 32 min at the equinoxes.

For the application of Eqs. (5.1)–(5.6), values of δ may be found in astronomical tables (e.g. List, 1966) or δ may be calculated from empirical expressions such as sin $\delta = a \sin[b + cJ + d \sin(e + cJ)]$, (5.7)

where J is the calendar day with $J = 1$ on January 1, and the constants are $a = 0.39785$; $b = 278.97$; $c = 0.9856$; $d = 1.9165$; $e = 356.6$ (Campbell and Norman, 1998).

Example.

Find the solar zenith angle at local solar noon, and the day length at Edinburgh, Scotland (55.0°N) on June 21 (calendar day 172).

Solution. Using astronomical tables or Eq. (5.7), the solar declination δ on June 21 is 23.5°. Equation (5.1) could be used to calculate the solar zenith angle ψ, but since the time is solar noon, when $\theta = 0$, the much simpler Eq. (5.3) applies, and

$\psi = \theta - \delta = 55.0 - 23.5 = 31.5°$

The day length is given by Eq. (5.6),

$2t = (24/\pi) \cos^{-1} (-\tan \phi \tan \delta)$,

$= (24/\pi) \cos^{-1} (-\tan 55.0 \tan 23.5)$,

$= (24/\pi) \cos^{-1} (-0.621) = 24 \times 2.24/\pi = 17.1$ h

(note that $\cos^{-1} (-0.621)$ is 2.24 radians).

3 Spectral Quality

For biological work, the spectrum of solar radiation can be divided into three major wavebands shown in Table 5.1 with the corresponding fraction of the TSI. Most measurements of solar energy at the ground are confined to the visible and near-infra-red wavebands which contain energy in almost equal proportions. **Table 5.1** Distribution of Energy in the Spectrum Emitted by the Sun.

Waveband (nm)	Energy (%)
0–200	0.7
200–280 (UV-C)	0.5
280–320 (UV-B)	1.5
320–400 (UV-A)	6.3
400–700 (visible/PAR)	39.8
700–1500 (near-infra-red)	38.8
1500 – ∞	12.4

Ultra-violet radiation contains sufficient energy per quantum to damage living cells. The ultra-violet spectrum is divided into UVA (320–400 nm) responsible for tanning the skin; UVB (280–320 nm) responsible for skin cancer and Vitamin D synthesis; and UVC (200–280 nm), potentially the most harmful waveband but absorbed almost completely by molecular oxygen in the stratosphere. Human skin is about 1000 times more sensitive to the UVB range than to the UVA. The waveband to which the eyes of humans and most terrestrial animals are sensitive ranges from blue (400 nm) through green (550 nm) to red (700 nm), with maximum sensitivity at around 500 nm. Eyes of aquatic mammals have peak sensitivity at slightly shorter wavelengths,

around 488 nm, perhaps a consequence of the ‒blueness" of the ocean habitat (Mcfarland and Munz, 1975). Eyes of fish have similar peak sensitivity.

Photosynthesis is stimulated by radiation in the samewaveband as human vision, and this waveband is referred to as *Photosynthetically Active Radiation* (PAR), a misnomer because it is green cells which are active, not radiation. Initially, the term PAR was applied to radiation measured in units of energy flux density (W m−2) but for two reasons it is more appropriately expressed as quantum flux density (mol m−2 s−1):

(i) when photosynthesis rates are compared for light of different quality (e.g. from the sun and from lamps), they are more closely related to the quantum content than to the energy content of the radiation (Jones, 1992) and (ii) because the number of moles of carbon dioxide fixed in photosynthesis is closely proportional to the number of moles of photons absorbed in the PAR waveband. The fraction of PAR to total energy in the extraterrestrial solar spectrum is about 0.40 (Table 5.1) but it is closer to 0.50 for solar radiation at the earth's surface (p. 68) because the atmosphere absorbs almost all the ultra-violet wavelengths and a significant part of the solar infra-red spectrum. Many developmental processes in green plants have been found to depend on the state of the pigment *phytochrome* which exists in two photo-interconvertible forms that absorb radiation in wavebands centered at 660 nm (red light—the Pr form) and 730 nm (far-red light—the Pfr form). The ratio of the two forms present in plant tissue changes in response to the ratio of spectral irradiance at these wavelengths, known as the red:far-red ratio (R:FR), so the phytochrome is an effective detector of the quality of radiation, for example detecting shading caused by other plants. *Shade avoidance* is one of the most important competitive strategies that plants possess. It consists of a range of physiological and developmental responses by plants that provides competitive advantages over other species when growing in the shade of other plants, e.g. weeds in crops or understory species in forest canopies. The responses may influence germination, stem elongation, leaf development, flowering, and reproduction. Shade avoidance responses are all initiated by a single environmental signal, a reduction in the ratio of red (R) to far-red (FR) (i.e. R:FR) radiation that occurs in crowded plant communities (Smith and Whitelam, 1997).

Attenuation of Solar Radiation in the Atmosphere

As the solar beam passes through the earth's atmosphere, it is modified in quantity, quality, and direction by processes of scattering and absorption (Figure 5.2).
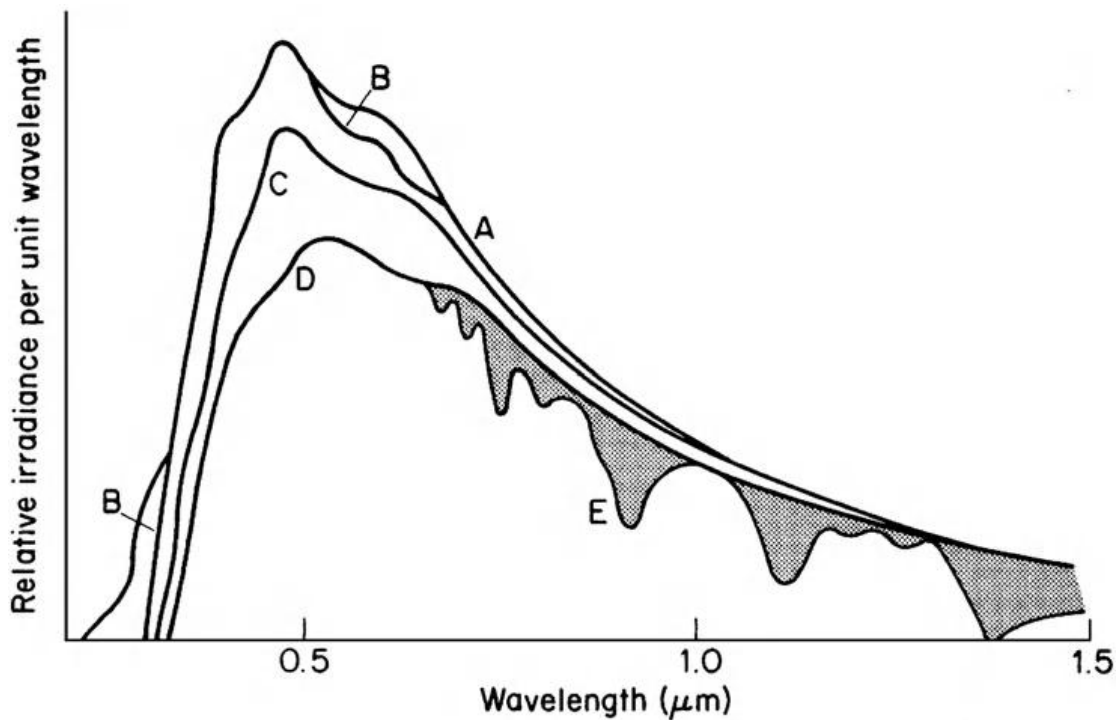
Figure 2 Successive processes attenuating the solar beam as it penetrates the atmosphere. A— extraterrestrial radiation, B—after ozone absorption, C—after molecular scattering, D—after aerosol scattering, E—after water vapor and oxygen absorption (from Henderson, 1977).

Scattering has two main forms. First, individual quanta striking molecules of any gas in the atmosphere are diverted in all directions, a process known as *Rayleigh scattering* after the British physicist who showed theoretically that the effectiveness of molecular scattering is proportional to the inverse fourth power of the wavelength. The scattering of blue light $(\lambda = 400$ nm*)* therefore exceeds the scattering of red (700 nm) by a factor of $(7/4)4$ or about 9. This is the physical basis of the blue color of the sky as seen from the ground and the blue haze surrounding the Earth when viewed from space. The redness of the sun's disk near sunrise or sunset is further evidence that blue light has been removed from the beam preferentially. Rayleigh also showed that the spatial distribution of scattered radiation was proportional to $(1 + \cos2 \ \theta)$, where

θ is the angle between the initial and scattered directions of the radiation. Thus the probability of forward- and backscattering is twice that at 90◦. Rayleigh scattering is confined to systems in which the diameter *(d)* of the scatterer is much smaller than the wavelength of the radiation λ. This condition is not met for particles of dust, smoke, pollen, etc., in the atmosphere, referred to as ‒aerosol," which often have diameters d in the range $0.1\lambda < d < 25\lambda$. The theory developed by Mie predicts that the wavelength dependence of scattering by aerosol particles should be a function of d/λ, and that, for some values of the ratio, longer wavelengths should be scattered more efficiently than short—the reverse of Rayleigh scattering. This happens rarely, but smoke with the appropriate narrow range of particle sizes, e.g. from forest fires, can occasionally cause the sun and moon viewed from the earth to appear blue! Usually, aerosol contains such a wide range of particle sizes that scattering is not strongly dependent on λ. Angstrom (1929) proposed that the dependence could often be described by a power law, i.e. $\propto \lambda^{-\alpha}$ where α had an average value of 1.3, and many investigators have confirmed the power law dependence. For example, a set of measurements in the English Midlands corresponded to α between 1.3 and 2.0 (McCartney and Unsworth, 1978). When particles are large and sufficiently dense for multiple scattering, there is essentially no wavelength dependence and the scattered light appears white, for example with very hazy skies in summer. Aerosol scattering is usually predominantly ‒forwards," i.e. in a narrow cone around the direction of the incident radiation.

Sources and Radioactive Properties of Aerosols

Aerosols are solid or liquid particles small enough to remain suspended in the atmosphere for long periods. They have an important *direct* influence on radiation reaching the ground because they scatter and absorb solar and long-wave radiation in the atmosphere, thus contributing to *radiative forcing* of the earth's energy budget. Aerosols also influence cloud albedo and duration by increasing the number of droplets in clouds and altering the efficiency of precipitation production, thus also having *indirect* effect on radiation (IPCC, 2007). These indirect effects are hard to isolate in the free atmosphere, but Coakley et al. (1987) demonstrated that they can be seen in ‒ship tracks" observed from space (Figure 3). When there is a thin layer of marine stratus cloud, the aerosols emitted from ships smokestacks increase the cloud density behind the vessel.

Aerosols in the lower atmosphere have relatively short lifetimes before they are removed by precipitation and turbulent transfer. Aerosols in the stratosphere, for example as a result of explosive volcanic eruptions, have much longer lifetimes and may be dispersed around the globe, causing observable effects on the earth's climate (Hansen et al., 2011).

The size distribution of aerosols is critical for their radiative effects. Particles in the ―accumulation size range" (Chapter 12) (i.e. with diameters between about 0.1 and 1.0 μm) scatter more light per unit mass than larger particles, and have longer lifetimes in the atmosphere, so are particularly important in influencing the irradiance at the ground. Some aerosols are *hygroscopic*, i.e. they absorb water depending on atmospheric humidity, thus changing the aerosol size distribution. Examples are sea-salt particles and ammonium sulfate.

Primary aerosols are generated at the surface by natural processes and human activity. Desert dust storms generate aerosols that can be transported across the Atlantic and Pacific oceans (Kaufman et al., 2002). Inefficient combustion of wood or fossil fuels releases organic and black carbon aerosols.

Secondary aerosols are created in the atmosphere by chemical reactions. An ubiquitous example is ammonium sulfate aerosol, formed by reactions that include the gases ammonia, sulfur dioxide, and dimethyl sulfide, which have natural sources (volcanoes, ocean plankton) and human sources (fossil fuel, animal production). Other secondary aerosols are created during photochemical smog episodes.

Absorption of radiation by aerosols is very variable. For example, desert dust may absorb little, but black carbon aerosols from wildfires and human activity are much stronger absorbers (Hansen et al., 2004). Absorption by secondary aerosols can be greatly increased when black carbon particles are incorporated into the aerosol. For several reasons, radiative effects of aerosols are generally much more difficult to assess than those of atmospheric gases: aerosols are not uniformly distributed, and may be formed and transformed in the atmosphere; some aerosol types (e.g. dust and sea salt) consist of particles whose physical properties that influence scattering and absorption have wide ranges; and aerosol species may combine to form mixed particles with optical properties different from their precursors. IPCC (2007) included a good review of progress in understanding aerosol effects on the earth's energy balance.

The second process of attenuation is *absorption* by atmospheric gases and aerosols. The most important gases absorbing solar radiation are ozone and oxygen (particularly in the ultra-violet spectrum), and water vapor and carbon dioxide (with strong bands in the infra-red). Absorption by aerosols is very variable, depending on the source of the material.

In contrast to scattering, which simply changes the direction of radiation, absorption removes energy from the beam so that the aerosol, and atmosphere containing it, is heated. In the ultra-violet, absorption by oxygen and ozone in the stratosphere removes.
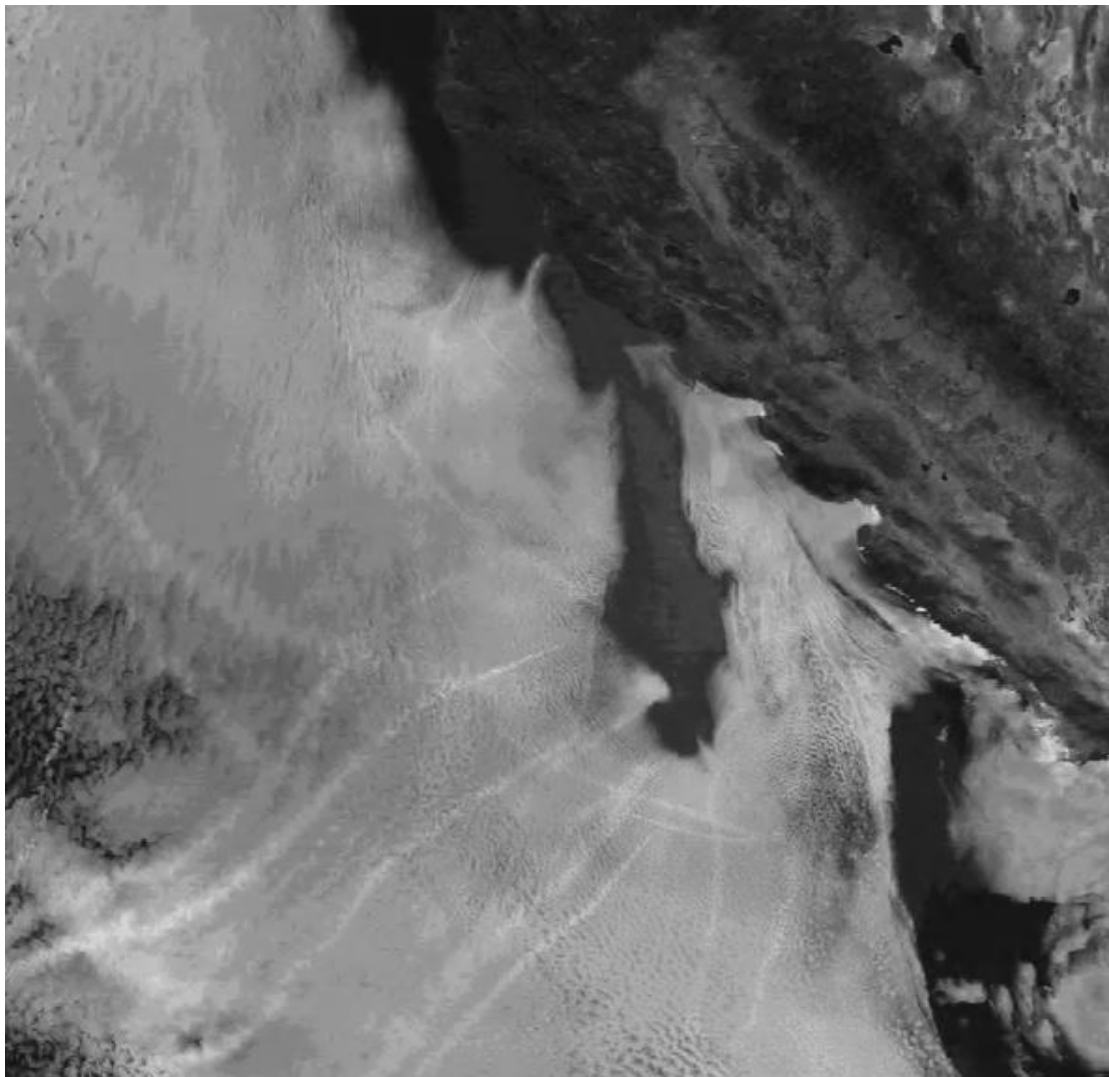
Figure 3 Infra-red satellite image of reflected solar radiation at 2.1μm off the coast of California near San Francisco. Pollution from ship smoke emissions increases the reflectivity of marine stratus clouds by supporting the formation of larger numbers of

smaller droplets than in unpolluted cloud nearby. This enables ship tracks to be seen clearly in the image. (Courtesy of Dr. J. A. Coakley)

All UVC and most UVB radiation before it reach the ground, resulting in stratospheric heating. The remaining UVB and UVA radiation is scattered very effectively however, so that it is possible to suffer serious sunburn beneath a cloudless sky even if not exposed to the direct solar beam.

In the visible region of the spectrum, absorption by atmospheric gases is much *less* important than molecular scattering in determining the spectral distribution of solar energy at the ground. In the infra-red spectrum, however, absorption is much *more* important than scattering, because several atmospheric constituents absorb strongly, notably water vapor with absorption bands between 0.9 and 3 μm. The presence of water vapor in the atmosphere thus increases the amount of visible radiation relative to infra-red radiation.

The scale of absorption and scattering in the atmosphere depends partly on the path length of the solar beam and partly on the amount of the attenuating constituent present in the path. The path length is usually specified in terms of an *air mass number m*, which is the length of the path relative to the vertical depth of the atmosphere. Air mass number therefore depends on altitude (represented by the pressure exerted by the atmospheric column above the site) and on zenith angle ψ. For values of zenith angle ψ less than 80°, the air mass number at a location where atmospheric pressure is P is simply

$m = (P/P_0)$ secψ, where P_0 is standard atmospheric pressure at sea level (101.3 kPa),

but for values between 80° and 90° ,m is smaller than secψ, because of the earth's curvature. Values, corrected for refraction, can be obtained from tables (e.g. List, 1966).

The most variable absorbing gas in the atmosphere is water vapor, the amount of which can be specified by a depth of *precipitable water u*, defined as the depth of water that would be formed if all the vapor were condensed (u is typically between 5 and 50 mm at most stations). If the precipitable water is u, the path length for water vapor is um. Similarly, the total amount of ozone in the atmosphere (the *ozone column*) is specified by an equivalent depth of the pure gas at a standard pressure of one atmosphere (101.3 kPa). At mid-latitudes, the ozone column is typically about 3 mm and varies only slightly with season. However over some parts of the Antarctic,

up to 60% of the ozone column is lost during the Antarctic Spring (September-October). When this phenomenon was first reported by Joe Farman of the British Antarctic Survey, who analyzed surface observations of irradiance in the UVB waveband (Farman et al., 1985), it could not be explained by atmospheric chemists and had not been detected by satellite monitoring. In retrospect, it turned out that a computer program had caused the anomalous Antarctic Spring data from the satellite to be ignored, and chemists traced the cause of the alarming decrease in ozone to the presence in the Antarctic stratosphere of frozen particles of nitric acid that served as catalytic sites for reactions destroying ozone. Figure 5.4 shows the decline of ozone column thickness from the mid-1950s in the Antarctic Spring. The extremely cold stratospheric conditions necessary for ozone destruction by this mechanism are less common over the Arctic, and fortunately do not exist over the large parts of the earth where plant and animal populations would be vulnerable to the extra UVB radiation that would reach the surface if ozone were depleted.

In contrast with the mainly regional effects of ozone depletion, the consequences of radiative absorption by the steadily increasing amount of carbon dioxide in the earth's atmosphere are apparent on a global scale as discussed in Chapter 2 and extensively reviewed by in Assessment Reports by the IPCC (2007).
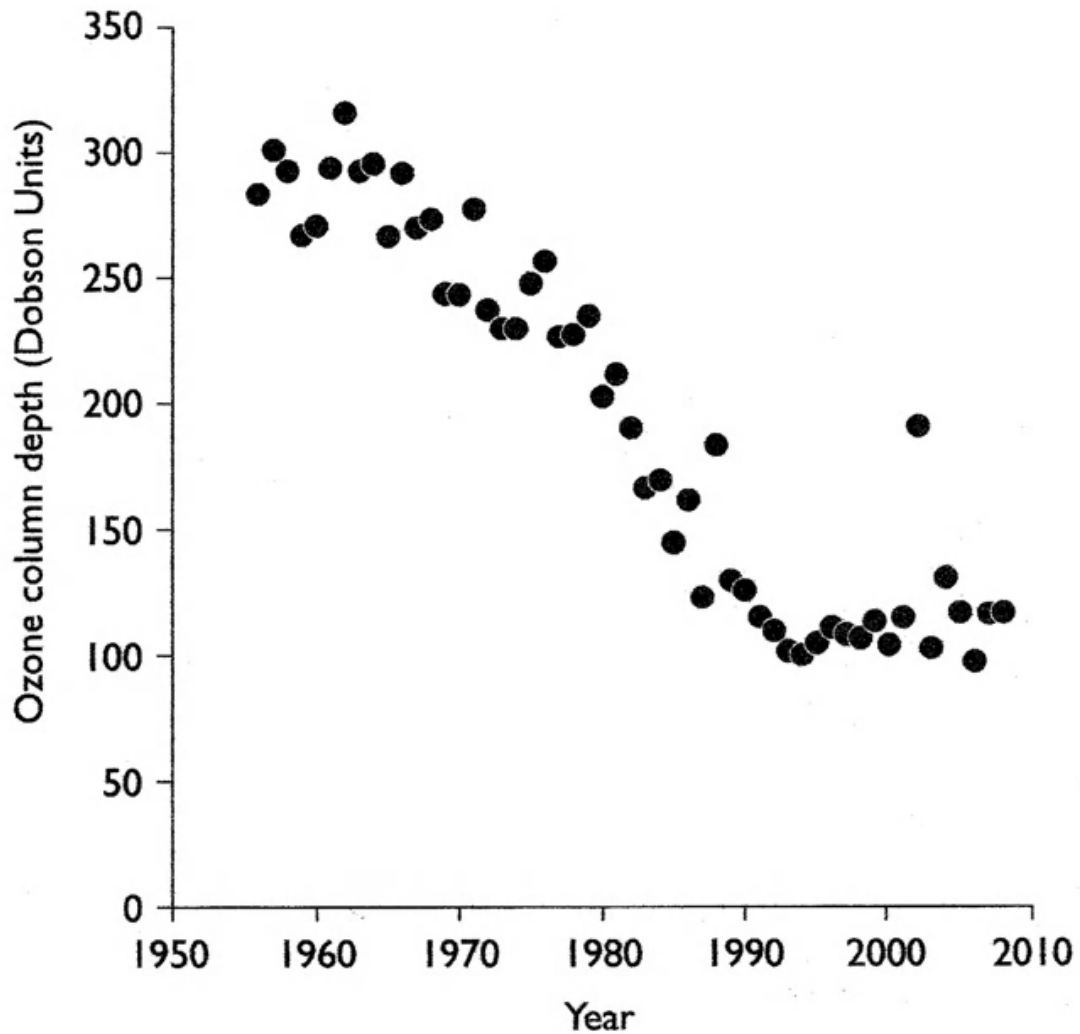
Figure 4 Minimum October ozone column depth at the British Antarctic Survey research station, Halley Bay, Antarctica from 1956 to 2009. (One Dobson Unit corresponds to a layer of gaseous ozone 10 μm thick at STP) (data courtesy of the British Antarctic Survey.)

Clouds, consisting of water droplets or ice crystals, scatter radiation both forwards and backwards, but when the depth of cloud is substantial, back-scattering predominates and thick stratus can reflect up to 70% of incident radiation, appearing snow-white from an aircraft flying above it. About 20% of the radiation may be absorbed, leaving only 10% for transmission, so that the base of such a cloud seems gray. However, at the edge of a cumulus cloud, where the concentration of droplets is small, forward scattering is strong—the silver lining effect—and under a thin sheet of cirrus the reduction of irradiance can be less than 30%, see Figure 10.

5.3 Solar Radiation at the Ground

As a consequence of attenuation, radiation has two distinct directional properties when it reaches the ground. *Direct* radiation arrives from the direction of the solar disk and includes a small component scattered directly forward. The term *diffuse* describes all other scattered radiation received from the blue sky (including the very bright aureole surrounding the sun) and from clouds, either by reflection or by transmission. The sum of the energy flux densities for direct and diffuse radiation is known as *total* or *global* radiation and for climatological purposes is measured on a horizontal surface. The symbols $\mathbf{S}b$, $\mathbf{S}d$, and $\mathbf{S}t$ describe direct, diffuse, and total irradiance, respectively, on a horizontal surface, and $\mathbf{S}p$ signifies direct irradiance measured at right angles to the solar beam.

Direct Radiation

At sea level, direct radiation $\mathbf{S}p$ rarely exceeds 75% of the Solar Constant i.e. about 1000 Wm−2. The minimal loss of 25% is attributable to molecular scattering and absorption in almost equal proportions with a negligible contribution from aerosol when the air mass is clean. Aerosol increases the ratio of diffuse to global radiation by forward scattering and changes the spectral composition. Several expressions are available to describe atmospheric transmissivity as affected by molecular and aerosol components. A simple practical relation is

$$\mathbf{S}p = \mathbf{S}*T\,m, \quad (5.8)$$

where $\mathbf{S}*$ is the Solar Constant (TSI), T is the *atmospheric transmissivity*, and m is the air mass number. Liu and Jordan (1960) found that T ranged from about 0.75 to 0.45 on cloudless days implying, as above, that aerosol attenuation was insignificant on the clearest days.

To illustrate more directly the combined impact of attenuation by aerosols and molecules, Beer's Law may be applied to give

$$\mathbf{S}p(\eta) = \mathbf{S}* \exp(-\eta m), \quad (5.9)$$

where η is an *extinction coefficient* or *optical thickness* and m is the air mass number. When the value of η is expressed as the sum of molecular extinction (η_m) and aerosol extinction (η_a), Eq. (5.9) may be written in the form

$$\mathbf{S}p(\eta) = \mathbf{S}* \exp(-\eta_m m) \exp(-\eta_a m) = \mathbf{S}p(0) \exp(-\eta_a m), \quad (5.10)$$

Where $\mathbf{Sp}(0)$ is the irradiance of the direct beam below an atmosphere free of aerosol. Comparison of Eqs. (5.8), (5.9), and (5.10) yields

$T = \exp\left(-\eta\right) = \exp\left(-(\eta_m m + \eta_a)\right)$ (5.11)

implying that η_m was about 0.3 in Liu and Jordan's measurements (assuming $\eta_a = 0$ when $T = 0.75$), and η_a was about 0.5 on the most turbid days that they recorded. The value of η_a at a site can be determined from Eq. (5.10) by measuring $\mathbf{Sp}(\eta)$ as a function of $m(=\sec\psi)$ and by calculating $\mathbf{Sp}(0)$ (also a function of m) from the properties of a clean atmosphere containing appropriate amounts of gases and water vapor. For example, a series of measurements in Britain gave values of η_a ranging from 0.05 for very clear air of Arctic origin to 0.6 for very polluted air in the English Midlands during a stagnant anticylone (Unsworth and Monteith, 1972). Corresponding values of $\exp\left(-\eta_a m\right)$ for $\psi = 30°$ are 0.92 and 0.50, indicating radiant energy losses of up to 50% from the direct solar beam due to aerosol scattering and absorption.

Using a bulk aerosol optical thickness such as η_a, determined from measurements of a broad waveband of solar radiation, is convenient when only standard radiometers are available. However, values of aerosol optical thickness derived from more sophisticated spectral observations in narrow wavebands are more commonly reported, e.g. for wavebands around 0.55 µm in the mid-visible spectrum (IPCC, 2007). Such values are generally consistent with η_a and are similar in magnitude because the solar spectrum peaks around 0.5 µm.
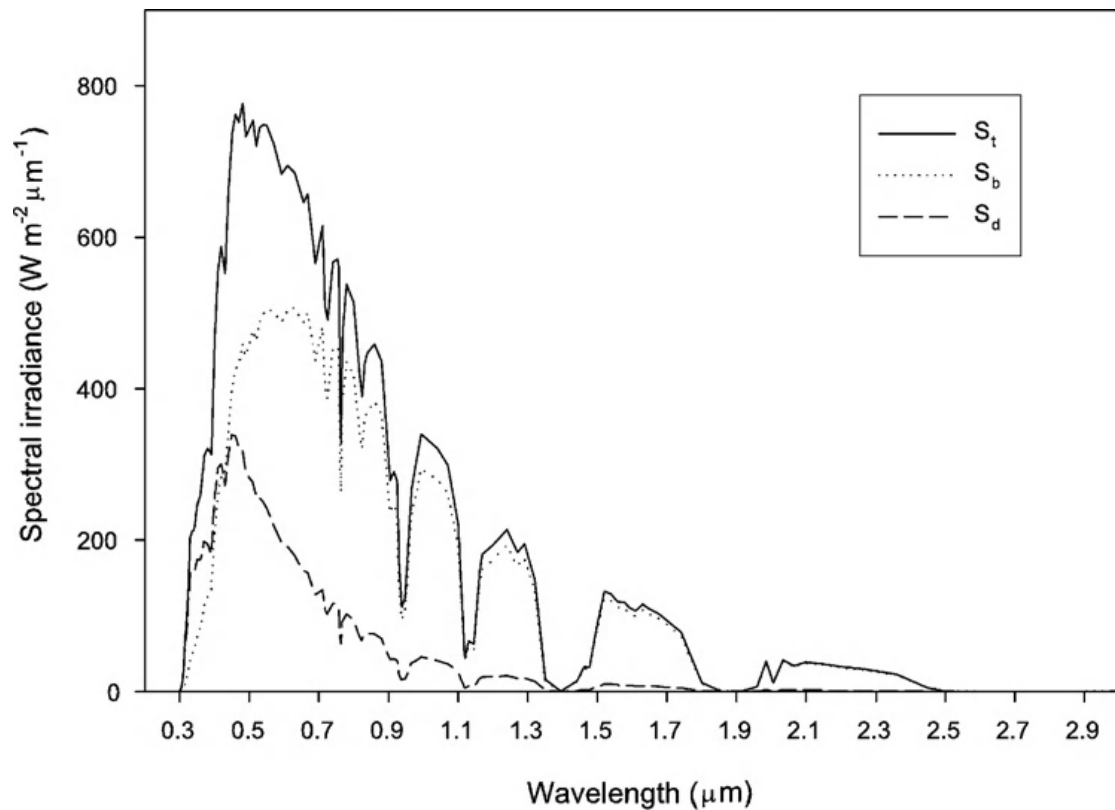
Figure 5 Spectral distribution of direct, diffuse, and total solar radiation calculated using a simple model of a cloudless atmosphere (courtesy of the Solar Energy Research Institute; see Bird and Riordan, 1984). Solar zenith angle is 60° *(m = 2)*, precipitable water is 20 mm, ozone thickness is 3 mm, and aerosol optical depth is 0.2. Note that the diffuse flux has maximum energy per unit wavelength at about 0.46 µm.

The spectrum of direct radiation depends strongly on the path length of the beam and therefore on solar zenith angle. A spreadsheet model for calculating direct and diffuse spectral irradiance (based on work by Bird and Riordan (1986))
 is available from the Solar Energy Research Institute, Golden, Colorado (http://rredc.nrel.gov/solar/models/spectral/). Figure 5 shows results at sea level calculated from the model, indicating that the spectral irradiance calculated for the solar beam is almost constant between 500 and 700 nm whereas, in the corresponding extraterrestrial spectrum, irradiance decreases markedly as wavelength increases beyond λm ≈ 500 nm (Figure2). The difference is mainly a consequence of energy removed from the beam by Rayleigh scattering which increases as wavelength decreases; ozone absorption is implicated too. As zenith angle increases, attenuation by scattering becomes very pronounced, and the wavelength for maximum direct solar

irradiance moves into the infra-red waveband when the sun is less than 20° above the horizon (see Figure 5).

The measurements by Unsworth and Monteith (1972) also showed that, for zenith angles between 40° and 60°, the ratio of visible to all-wavelength radiation in the direct solar beam decreased from a maximum of about 0.5 in clean air to about 0.4 in very turbid air. The maximum ratio exceeds the figure of 0.40 for extraterrestrial radiation (Table 5.1) because losses of visible radiation by scattering are more than offset by losses of infra-red radiation absorbed by water vapor and oxygen (Figure 2). McCartney (1978) found that the quantum content of *direct* radiation increased with turbidity from a minimum of about 2.7 μmol J−1 total radiation in clean air to about 2.8 μmol J−1 in turbid air. Theoretical values can be calculated using the spectral irradiance model referred to above (Confusion has arisen in the literature Radiation where quantum content values for *direct* radiation are compared with values referring to *global* radiation, as given later.)

2 Diffuse Radiation

Beneath a clean, cloudless atmosphere, the diffuse irradiance $\mathbf{S}d$ reaches a broad maximum somewhat less than 200Wm−2 when ψ is less than about 50°, and the ratio of diffuse to global irradiance then falls between 0.1 and 0.15. As turbidity increases, so does $\mathbf{S}d/\mathbf{S}t$, and for ψ <60°, observations in the English Midlands fit the relation

$\mathbf{S}d/\mathbf{S}t = 0.68\eta a + 0.10.$ (5.12)

For ψ > 60°

, $\mathbf{S}d/\mathbf{S}t$ is also a function of ψ and is larger than Eq. (5.12) predicts.

With increasing cloud amount also, $\mathbf{S}d/\mathbf{S}t$ increases and reaches unity when the sun is obscured by dense cloud: but the absolute level of $\mathbf{S}d$ is maximal when cloud cover is about 50%. The spectral composition of diffuse radiation is also strongly influenced by cloudiness. Beneath a cloudless sky, diffuse radiation is predominantly within the visible spectrum (Figure 5.4) but as cloud increases, the ratio of visible/all-wavelength radiation decreases toward the value of about 0.5 characteristic of global radiation.

3 Angular Distribution of Diffuse Radiation

Under an overcast sky, the flux of solar radiation received at the ground is almost completely diffuse. If it were perfectly diffuse, the radiance of the cloud base

observed from the ground would be uniform and would therefore be equal to Sd/π from Eq. (4.8).

The source providing this distribution is known as a *Uniform Overcast Sky* (UOS). In practice, the average radiance of a heavily overcast sky is between two and three times greater at the zenith than the horizon (because multiple-scattered radiation is attenuated by an air mass depending on its perceived direction and so regions near the horizon appear relatively depleted). To allow for this variation, ambitious architects and pedantic professors describe the radiance distribution of overcast skies as a function of zenith angle given by

$N(\psi) = N(0)(1 + b \cos \psi)/(1 + b).$ (5.13)

This distribution defines a *Standard Overcast Sky*. Measurements indicate that the number $(1 + b)$ which is the ratio of radiance at the zenith to that at the horizon is typically in the range 2.1–2.4 (Steven and Unsworth, 1979), values supported by theoretical analysis (Goudriaan, 1977) which also shows the dependence on surface reflectivity. The value $(1 + b) = 3$, in common use, is based on photometric studies and significantly overestimates the diffuse irradiance of surfaces.

Under a cloudless sky, the angular distribution of skylight depends on the position of the sun and cannot be described by any simple relation. In general, the sky round the sun is much brighter than elsewhere because there is a preponderance of scattering in a forward direction but there is a sector of sky about 90_ from the sun where the intensity of skylight is below the average for the hemisphere (Figure 6). On average, the diffuse radiation from a blue sky tends to be stronger nearer the horizon than at the zenith. As the atmosphere becomes more dusty, the general effect is to reduce the radiance of the circumsolar region and to increase the relative radiance of the upper part of the sky at the expense of regions near the horizon. Consequently the angular distribution of radiance becomes more uniform as turbidity increases.
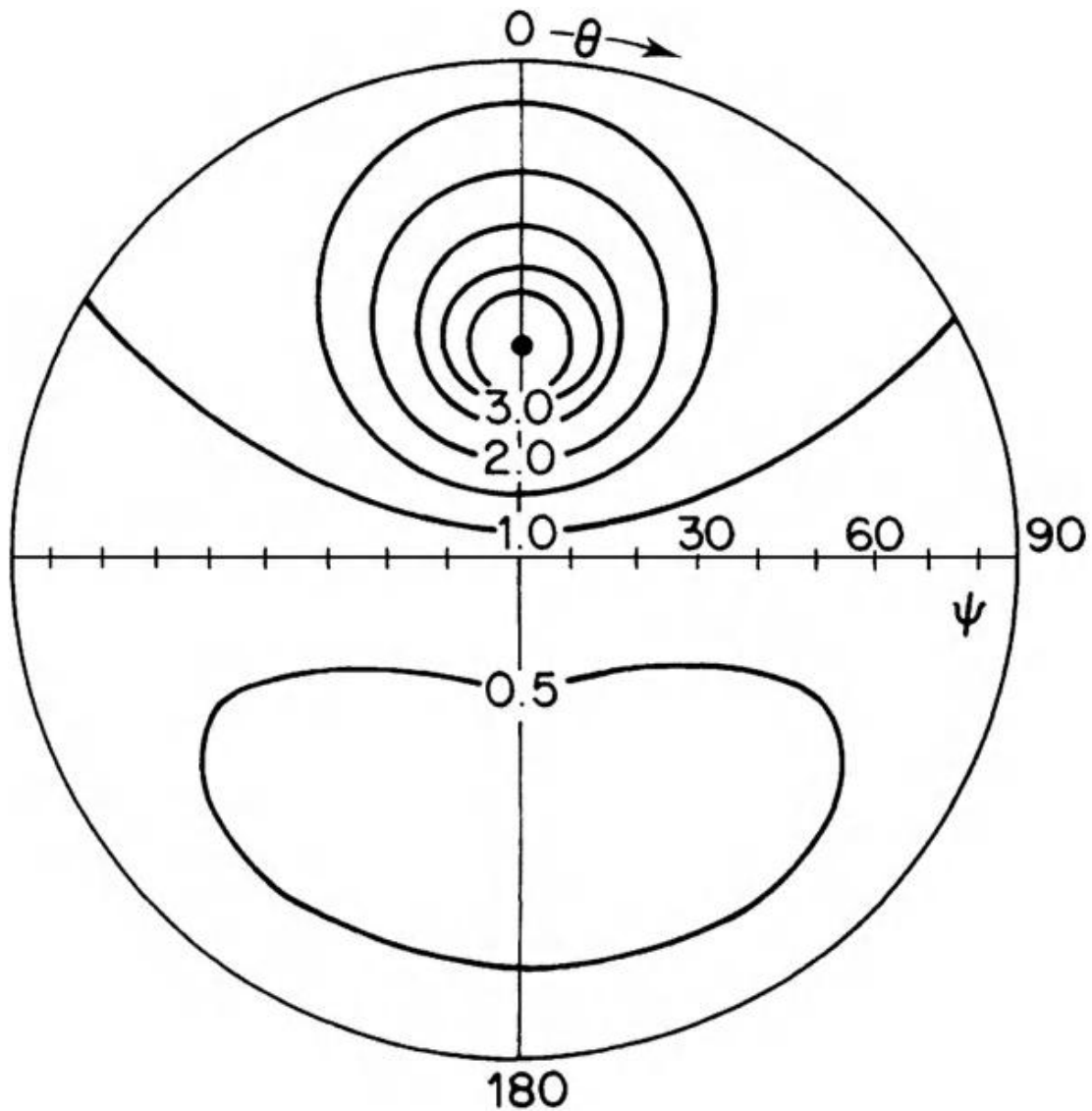
Figure 6 Standard distribution of normalized sky radiance $\pi N/Sd$ for solar zenith angle 35°, where **N** is the value of sky radiance at a point and πN is the diffuse flux which the surface would receive if the whole sky were uniformly bright (see p. 46) (from Steven, 1977).

5.3.4 Total (Global) Radiation

The total (global) radiation on a horizontal surface is given formally by

$St = Sp \cos\psi + Sd$

$= Sb + Sd,$ (5.14)

where $Sb = Sp \cos\psi$ is the contribution from the direct beam.

Figure 7 contains an example of measured values of **St**, **Sd**, and **Sb** as a function of solar zenith angle at Sutton Bonington, England, and Figure 5.8 shows similar data (with the addition of **Sp***)* from a more southerly site at Eugene, Oregon. **Estimating**

Irradiance Under Cloudless Skies A simple spreadsheet model that enables calculations of **Sp**, **Sd**, and **St** under cloudless skies at any location and date for specified values of water vapor, ozone
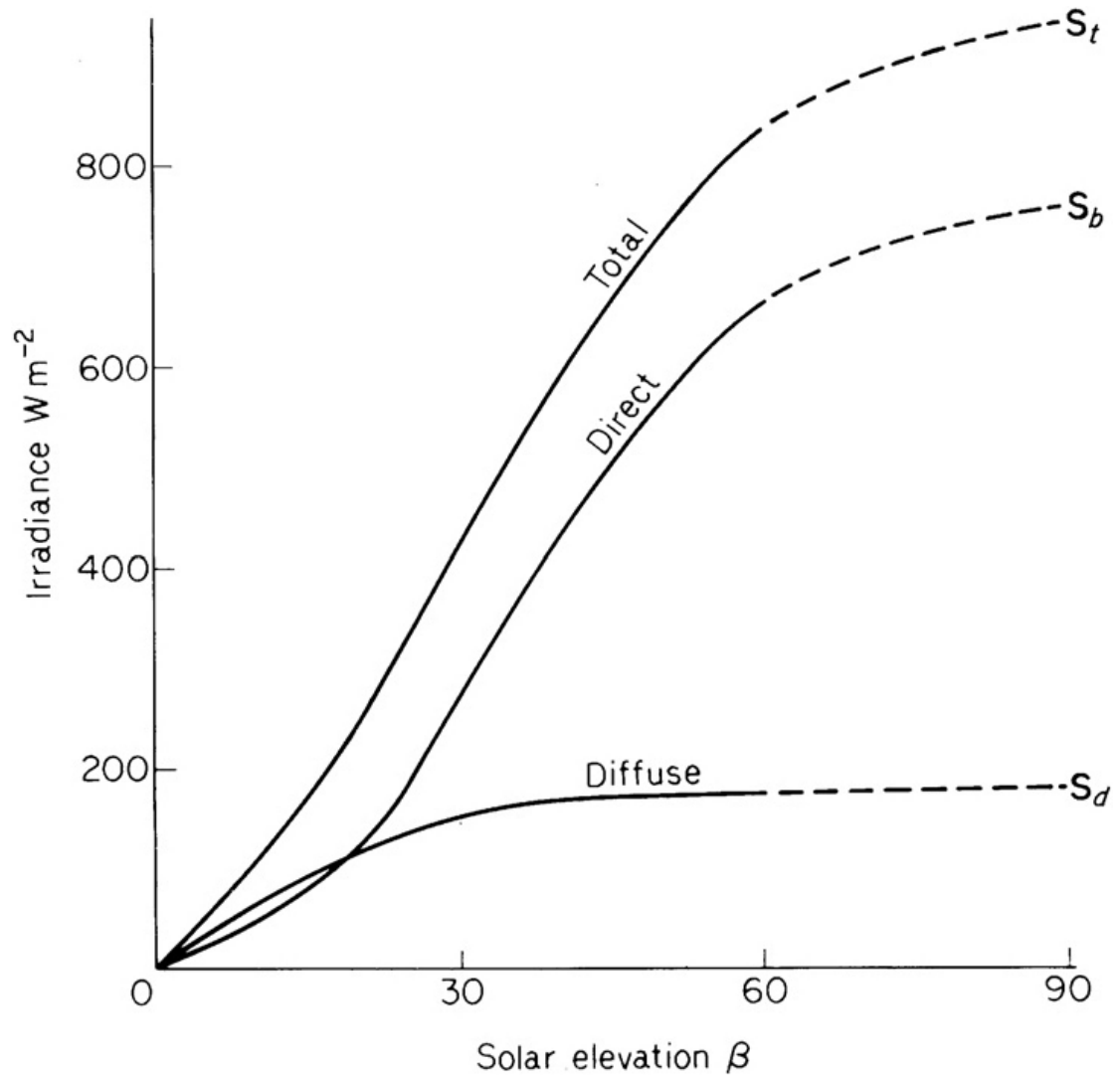
Figure 7 Solar irradiance on a cloudless day (16 July 1969) at Sutton Bonington (53∘N, 1∘W): **St** total flux; **Sd** diffuse flux, **Sb** direct flux on a horizontal surface.
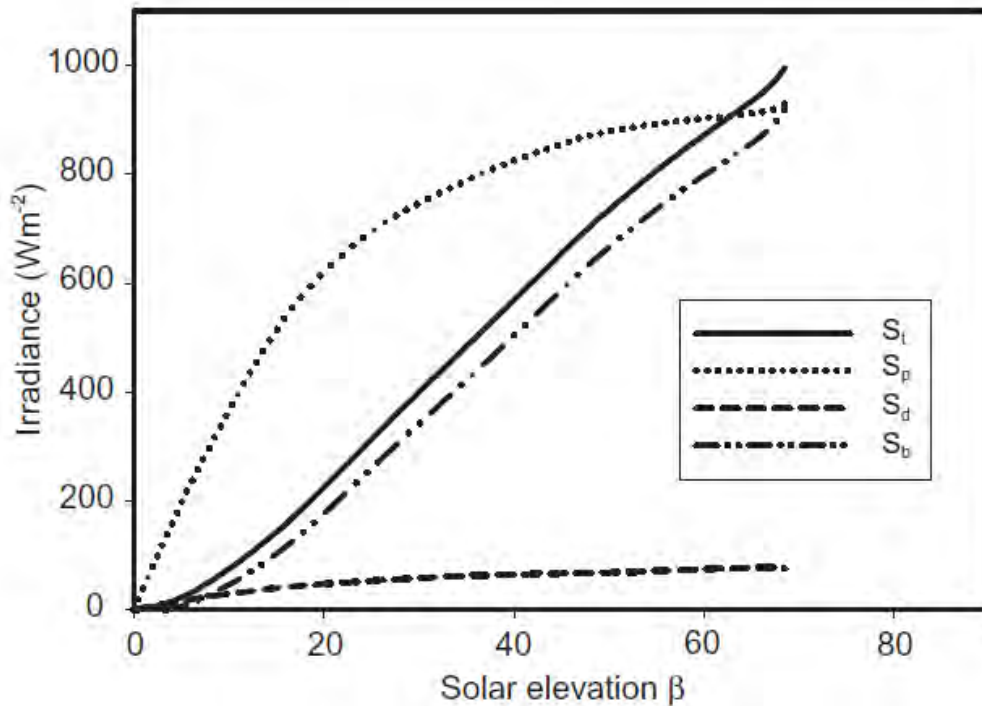
Figure 8 Solar irradiance on a cloudless day (12 June 2002) at Eugene, Oregon (44◦N, 123◦W): **St** total flux; **Sp** direct flux at normal incidence; **Sd** diffuse flux; **Sb** direct flux on a horizontal surface. (data courtesy of Frank Vignola, University of Oregon.) and aerosol optical thickness is based on the work of Bird and Hulstrom (1981)

and is available from the Solar Energy Research Institute, Golden, Colorado (http://rredc.nrel.gov/solar/models/clearsky/). The following simpler approach for direct and diffuse (and hence total) radiation gives estimates of appropriate accuracy for biological calculations. Using Eq. (5.10), it can be shown that

$$\textbf{Sp} = \textbf{S} \ast \exp{(-\eta_m m)} \exp{(-\eta_a m)}. \quad (5.15)$$

The Solar Constant **S**∗ is 1361Wm−2 (Section 5.1.1), the optical thickness for molecular attenuation η_m is typically about 0.3 (but changes with the amount of water vapor and other absorbing gases in the atmosphere), and the aerosol optical thickness η_a is typically in the range 0.05–0.50. Given appropriate values of these parameters, **Sp** can be calculated for a specific air mass number m (where the dependence of m on solar zenith angle ψ is given by $m = (P/P0)\sec\psi$ (p. 56).

Approximate values of **Sd** as a function of m on cloudless days can be estimated from an empirical equation based on measurements by Liu and Jordan (1960), i.e.

$$\textbf{Sd} = 0.3 S\ast[1 - \exp{(-(\eta_m + \eta_a)m}] \cos{\psi}. \quad (5.16)$$

The total irradiance is then given by

$S_t = S_p \cos\psi + S_d.$
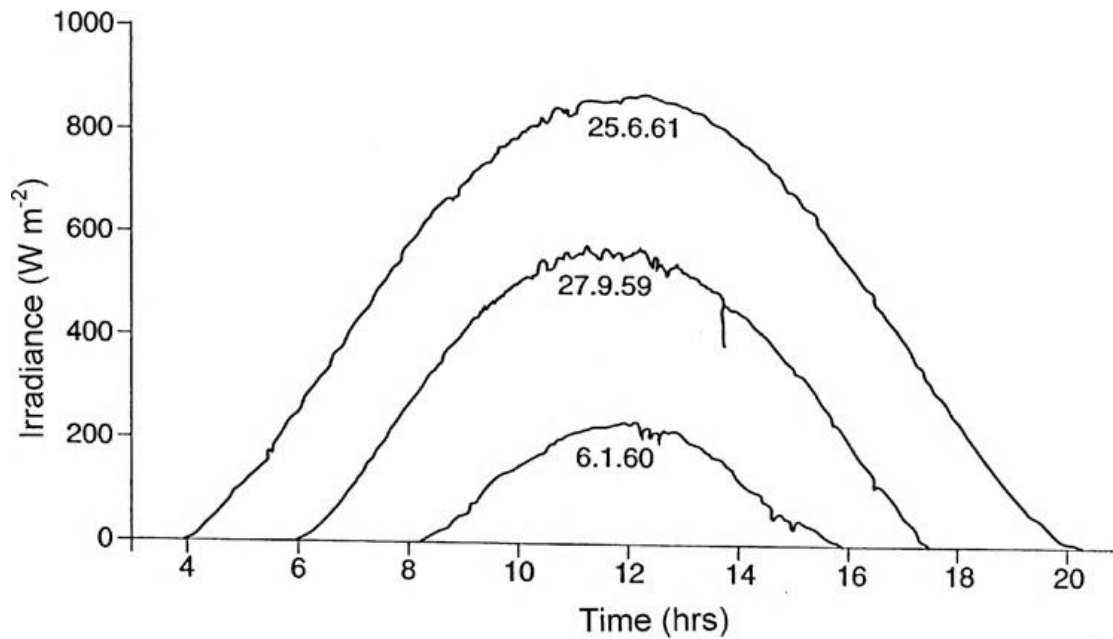
Figure 9 Solar radiation on three cloudless days at Rothamsted, England (52°N, 0°W).During the middle of the day, the record tends to fluctuate more than in the morning and evening, suggesting a diurnal change in the amount of dust in the lower atmosphere, at least in summer and autumn.

On cloudless days, illustrated in Figure 5.9, the change of S_t with time is approximately sinusoidal. This form is distorted by cloud, but in many climates the degree of cloud cover, averaged over a period of a month, is almost constant throughout the day so the monthly average variation of irradiance over a day is again sinusoidal. In both cases, the irradiance at t hours after sunrise can be expressed as

$S_t = S_{tm} \sin(\pi t/n),$ (5.17)

where S_{tm} is the maximum irradiance at solar noon and n is the day length in hours. This equation can be integrated to give an approximate relation between maximum irradiance and the daily integral of irradiation (the *insolation*) by writing

$$\int_0^n S_t dt \approx 2S_{tm} \int_0^{n/2} \sin(\pi t/n)dt = (2n/\pi)S_{tm}.$$

For example, over southern England in summer, S_{tm} may reach $900 Wm^{-2}$ on a clear cloudless day and with $n = 16 h = 58 \times 10^3 s$, the insolation calculated from equation (5.18) is 33 MJ m^{-2} compared with a measured maximum of about 30 MJ m^{-2}. In Israel, where S_{tm} reaches $1050 Wm^{-2}$ in summer for a day length of 14 h, the equation gives an insolation of 34MJ m^{-2} compared with 32 MJ m^{-2} by measurement.

At higher latitudes in summer when dawn and dusk are prolonged, a full sine wave may be more appropriate than Eq. (5.18). If S_t is given by

$S_t \approx S_{tm}(1 - \cos 2\pi t/n) = S_{tm} \sin^2 (\pi t/n)$ (5.19)

integration yields

$$\int_0^n S_t dt = S_{tm} n/2.$$

showed that the radiation regime at Aberdeen (57°N) was described best by the average of values given by Eqs. (5.18) and (5.20).

In most climates, the daily receipt of total solar radiation is greatly reduced by cloud for at least part of the year. Figure 5.10 shows the extent to which the total irradiance beneath continuous cloud depends on cloud type and solar elevation $\beta(=\pi/2 - \psi)$.

The fraction of extraterrestrial radiation can be read from the full lines and the corresponding irradiance by interpolation between the dashed lines.

The formation of a small amount of cloud in an otherwise clear sky always increases the diffuse flux but the direct component remains unchanged provided neither the sun's disk nor its aureole is obscured. With a few isolated cumuli, the total irradiance can therefore exceed the total irradiance beneath a cloudless sky by 5–10%. On a day of broken cloud (Figure 5.11), the temporal distribution of radiation is strongly bimodal:

the irradiance is very weak when the sun is completely occluded and strong when it is exposed. For a few minutes before and after occlusion, the irradiance commonly reaches $1000 Wm^{-2}$ in temperate latitudes and even exceeds the Solar Constant in the tropics. This effect is a consequence of strong forward scattering by the small concentration of water droplets present at the edge of a cloud.
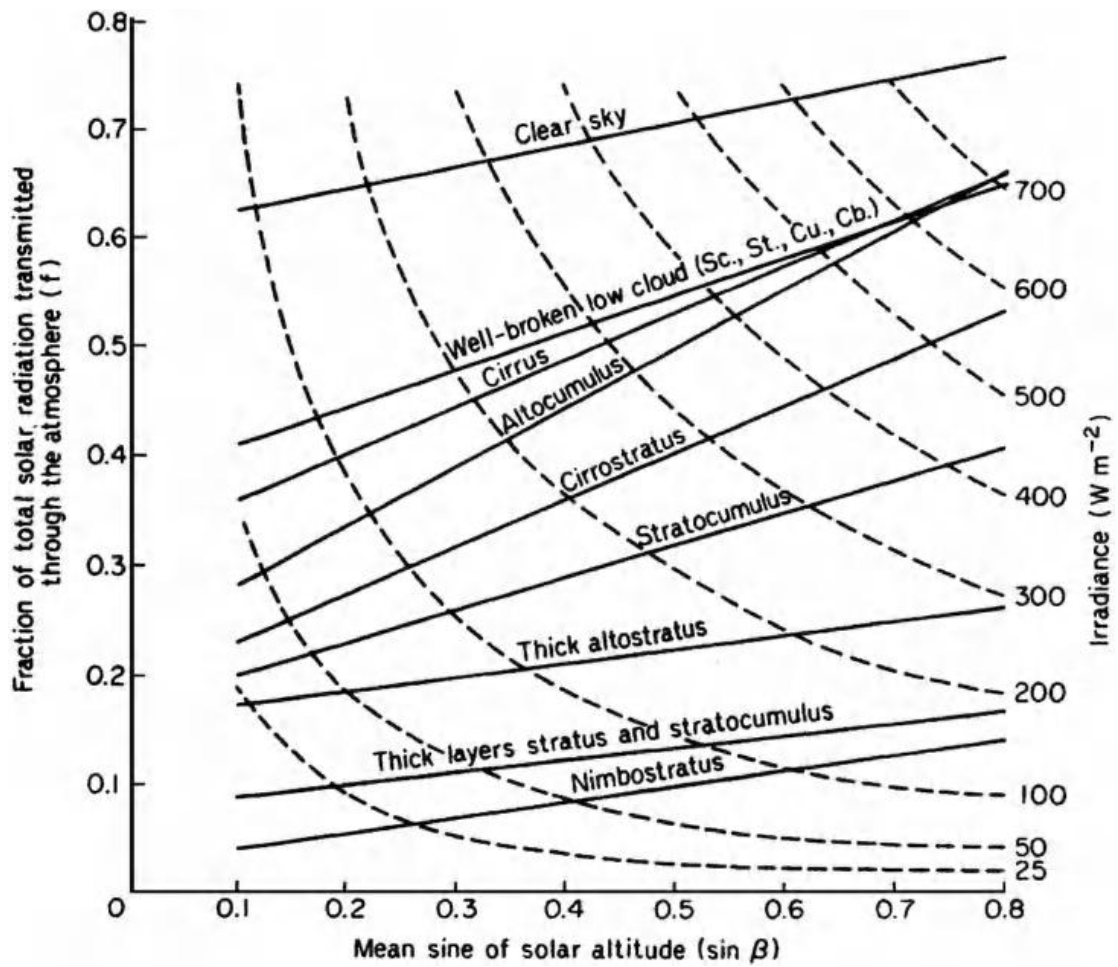
Figure 10 Empirical relations between solar radiation and solar angle for different cloud types from measurements in the North Atlantic (52◦N, 20◦W). The curves are isopleths of irradiance (from Lumb, 1964). Sc, stratocumulus; St, stratus; Cu, cumulus; Cb, cumulonimbus.
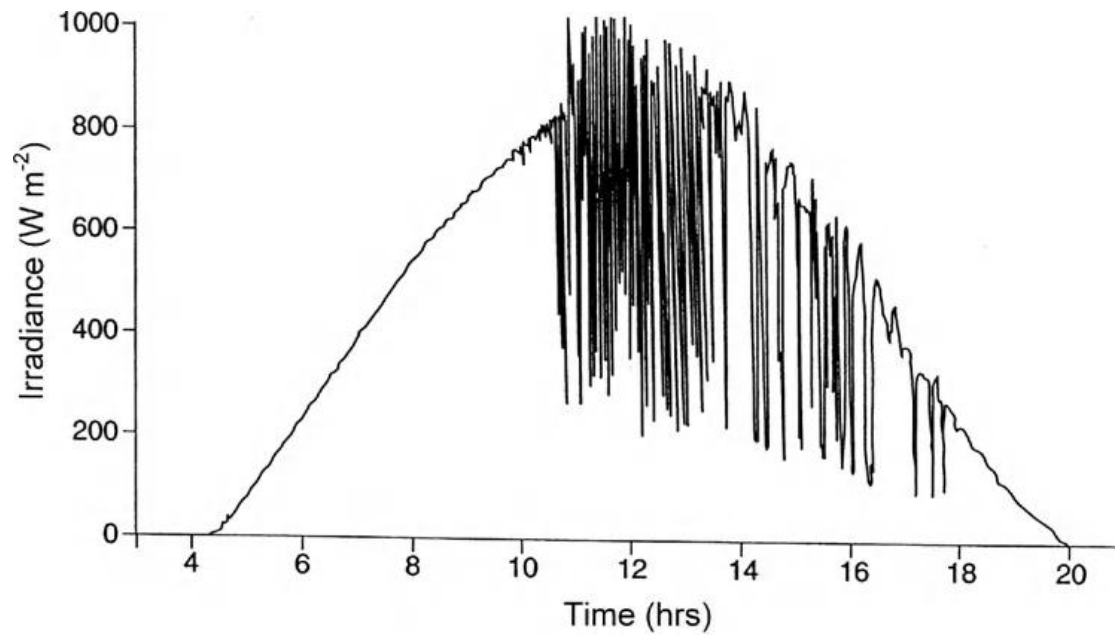
Figure 11 Solar radiation on a day of broken cloud (11 June 1969) at Rothamsted, England (52∘N, 0∘W). Note very high values of irradiance immediately before and after occlusion of the sun by cloud and the regular succession of minimum values when the sun is completely obscured.

As a consequence of cloud, the average insolation over most of Europe in summer is restricted to between 15 and 25 MJ m−2, about 50–80% of the insolation on cloudless days. Comparable figures in the USA range from 23 MJ m−2 round the Great Lakes to 31 MJ m−2 under the almost cloudless skies of the Sacramento and San Joaquin valleys
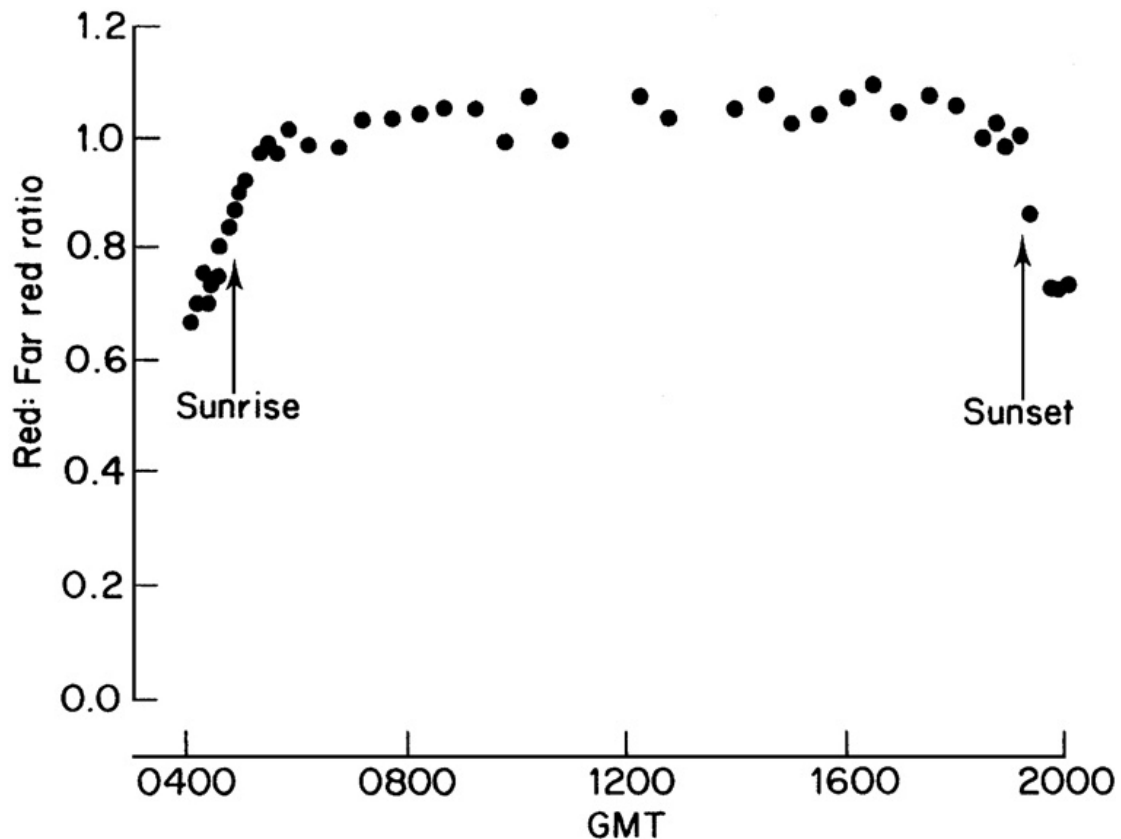
Figure 12 Ratio of spectral irradiance at 660 nm (red) to irradiance at 730 nm (far-red) on an overcast day (25 August 1980) near Leicester in the English Midlands (from Smith and Morgan, 1981).

Winter values range from 1 to 5MJ m−2 over most of Europe and from 6 MJ m−2 in the northern USA to 12 MJ m−2 in the south. Australian stations record a range of values similar to those of the USA.

The energy efficiency of photovoltaic solar panels is defined as the ratio of the electrical power produced by the panel to the radiative power falling on the panel. Commercial flat panels typically achieve a maximum efficiency of about 20%. That is, if the incident irradiance on a panel of area 1 m2 is 1 kW the maximum power output would be 200W.

Although the difference of irradiance with and without cloud is roughly an order of magnitude, the radiation to which plants are exposed covers a much wider range. In units of micromoles of photons m−2 in the PAR waveband, full summer sunshine is approximately 2200, shade on a forest floor 20, twilight 1, moonlight 3×10−4, and radiation from an overcast sky on a moonless night about 10−7 (Smith and Morgan, 1981).

At any location, annual changes of insolation depend in a complex way on seasonal changes in the water vapor and aerosol content of the atmosphere and on the seasonal distribution of cloud. Table 5.2 shows the main components of attenuation for four "seasons" at Kew Observatory, a suburban site 10 miles (16 km) west of the center of London. The data were collected in the 1950s when London air was more heavily polluted with smoke particles from inefficiently burned coal than it is now, so the "dust and smoke" losses for winter are relatively large. For the annual average, roughly a third of the radiation received outside the atmosphere is scattered back to space, a third is absorbed, and a third is transmitted to the surface. The flux at the surface is 20–25% less than it would be in a perfectly clear atmosphere. Because the climate at Kew is relatively cloudy, the diffuse component is larger than the direct component throughout the year.

Table 5.2 Short-Wave Radiation Balance of Atmosphere and Surface at Kew Observatory (51.5°N) for 1956–1960 Expressed as a Percentage of Extraterrestrial Flux

	Winter (Nov–Jan)	Spring (Feb–Apr)	Summer (May–Jul)	Autumn (Aug–Oct)	Year
Extraterrestrial radiation (ET)					
Seasonal total (MJ m^{-2})	800	2050	3720	2340	8910
Daily mean (MJ m^{-2} day^{-1})	8.7	22.3	40.4	25.4	24.4
Losses in the atmosphere (%ET)					
(a) Absorption					
Water vapor	15	12	13	15	13
Cloud	8	9	9	9	9
Dust and smoke	15	10	5	8	8
Total	38%	31%	27%	32%	30%
(b) Scattering (away from surface)	37%	35%	33%	34%	34%
Radiation at surface (%ET)					
Direct	8	14	18	14	15
Diffuse	17	20	22	20	21
Total	25%	34%	40%	34%	36%
	100%	100%	100%	100%	100%
Total as MJ m^{-2} day^{-1}	2.2	7.6	16.2	8.7	8.8

Spectrum of Total Solar Radiation

The spectrum of global solar radiation depends, in principle, on solar zenith angle, cloudiness, and turbidity and the interaction of these three factors limits the usefulness of generalizations. As zenith angle increases beyond 60◦, so does the proportion of scattered radiation and therefore the ratio of visible to all-wavelength radiation. In one record from Cambridge, England, this ratio increased from about 0.49 at $\psi = 60◦$ to 0.52 at $\psi = 10◦$ (Szeicz, 1974). Cloud droplets absorb radiation in the infra-red spectrum, so with increasing cloud the fraction of visible radiation should increase.

Again at Cambridge, the range was between 0.48 in summer and 0.50 in winter. Finally, with increasing turbidity, shorter wavelengths are scattered preferentially, depleting the direct beam but contributing to the diffuse flux so that the change in global radiation is relatively small. In another set of measurements at a site close to Cambridge, the visible: all-wavelength ratio decreased from 0.53 at $\eta a = 0.1$ to 0.48 at $\eta a = 0.6$ (McCartney, 1978). Elsewhere, a smaller value of the ratio, 0.44, with little seasonal variation was reported for a Californian site by Howell et al. (1983) and, in the tropics, Stigter and Musabilha (1982) found that the ratio increased from 0.51 with clear skies to 0.63 with overcast. It is probable that some of the apparent differences between sites reflect differences or errors in instrumentation and technique rather than in the behavior of the atmosphere.

At a given site, the relation between quantum content and energy appears to be conservative. McCartney (1978) reported a value of 4.56 ± 0.05 μmol J−1 (PAR) in the English Midlands. This is equivalent to about 2.3 μmol J−1 total (global) radiation but other values reported range from 2.1 μmol J−1 in California to 2.9 μmol J−1 in Texas (Howell et al., 1983). The ratio of quantum content to energy in the PAR wave band for diffuse radiation from a cloudless sky is smaller than that for total radiation, about 4.25 μmol J−1 PAR, because quanta at shorter wavelengths carry more energy than those at longer wavelengths.

The ratio of energy per unit wavelength in red and far-red wavebands is also conservative and has a value of about 1.1 during the day when solar elevation exceeds 10◦ (Figure 11). Thus the ratio of the red to far-red forms of phytochrome in plants is constant through the day unless shading by other vegetation occurs (see p. 53). As the sun approaches the horizon, the ratio decreases because red light is scattered more than far-red and because only a small fraction of the forward-scattered light reaches the ground. There is some evidence that the ratio starts to increase and returns to

values greater than 1 when the solar disk falls below the horizon, presumably because skylight alone is relatively rich in shorter wavelengths (Figure 5).

Terrestrial Radiation

At the wavelengths associated with solar radiation, emission from radiatively active gases in the earth's atmosphere, and from the earth's surface is negligible, so the previous section considered only absorption and scattering. In contrast, at wavelengths of terrestrial radiation (i.e. long-wave radiation originating in the earth's atmosphere and at its surface), both absorption and emission are important and will be considered in this section.

Most natural surfaces can be treated as ―full" radiators which emit long-wave radiation, in contrast to the short-wave solar radiation emitted by the sun. At a surface temperature of 288 K, the energy per unit wavelength of terrestrial radiation (based on Wien's Law, p. 39) reaches a maximum at 2897/288 or 10 μm, and arbitrary limits of 3 and 100 μm are usually set for the long-wave spectrum. Figure 5.13 illustrates the spectrum of radiation that would be emitted to the atmosphere from a surface that was a full radiator at 288 K.

In the absence of cloud, most of the radiation emitted by the earth's surface is absorbed within the atmosphere in specific wavebands by radiatively active atmospheric gases, mainly water vapor and carbon dioxide. A small fraction of radiation from the surface escapes to space, mostly through the *atmospheric window* between 8 and 12 μm. The energy absorbed in atmospheric gases is re-radiated (emitted) in all directions. Atmospheric gases do not emit like full radiators: rather, they have an emission spectrum similar to their absorption spectrum (Kirchhoff's principle, p. 38). Figure 13 shows the approximate spectral distribution of the downward flux of atmospheric radiation that would be received at the earth's surface from a cloudless atmosphere at 263 K. In reality, much of the atmospheric radiation that reaches the surface arises from gases close to the surface, and consequently close to surface temperature: atmospheric
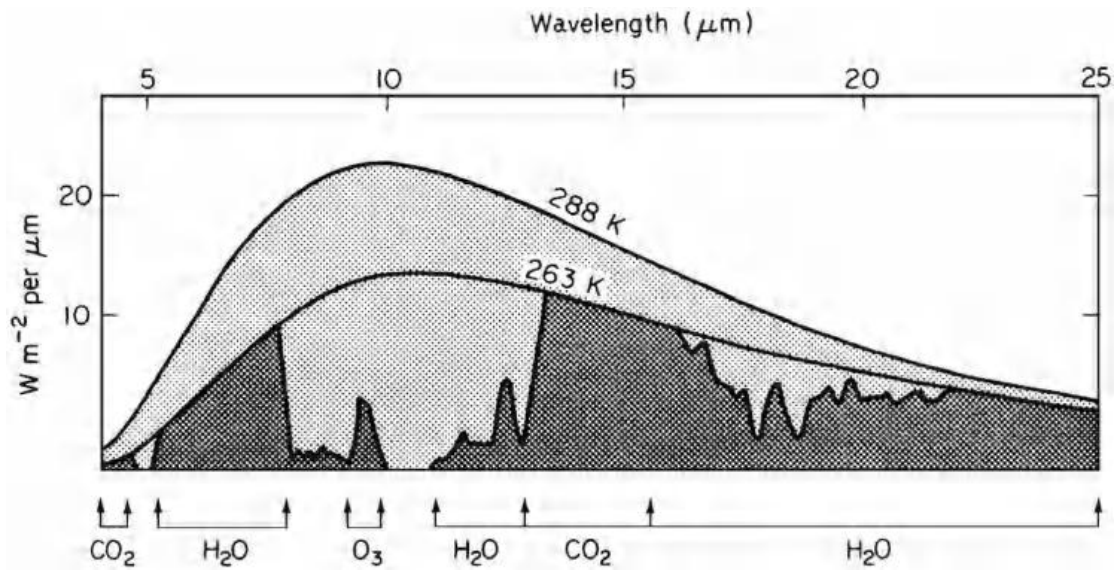
Figure 5.13 Spectral distribution of long-wave radiation for black bodies at 298 K and 263 K. Dark gray areas show the emission from atmospheric gases at 263 K. The light gray area therefore shows the net loss of radiation from a surface at 288 K to a cloudless atmosphere at a uniform temperature of 263 K (after Gates, 1980).

radiation that is lost to space is emitted mainly from gases higher in the troposphere where temperatures are less. Radiation emitted to space is therefore partly surface emission, escaping through the atmospheric window, and partly atmospheric emission from the upper troposphere and stratosphere.

To satisfy the First Law of Thermodynamics for the earth as a planet, assuming that the earth is in equilibrium, the average annual loss of long-wave radiative energy to space must balance the average net gain from solar radiation. If rE is the radius of the earth, $\mathbf{S}*$ is the Solar Constant, ρE is the planetary albedo (the fraction of solar radiation scattered to space from clouds and the surface), and $\mathbf{L}$ is the emitted radiative flux density (emittance) to space, this balance may be expressed as

$(1 - \rho E)\mathbf{S}* \pi r 2E = 4\pi r 2E \ \mathbf{L}$ (5.21)

or

$\mathbf{L} = (1 - \rho E)\mathbf{S}* /4.$

Taking ρE = 0.30 and $\mathbf{S}* = 1361 Wm-2$ yields $\mathbf{L} = 238 Wm-2$, and using the Stefan-Boltzmann Law(Eq. 4.2) this corresponds to an equivalent black-body temperature of the earth viewed from space of 254 K (−19 ∘C). The low value in comparison to the mean temperature at the surface (about 288 K, 15 ∘C) is an indication of the extent to

which atmospheric gases and cloud create a favorable climate for life on earth. This phenomenon is commonly called the *greenhouse effect,* though the term is a poor one, as real greenhouses become warm by reducing heat loss by the wind and convection rather than primarily by radiative effects. In fact, the assumption of radiative equilibrium for the earth is incorrect: the earth is currently experiencing additional *radiative forcing* (i.e. absorption of radiation) of about 1.6Wm−2 relative to pre-industrial times as a consequence of human activities, primarily emissions of greenhouse gases (IPCC, 2007), and this is causing *global warming.* If human perturbations of the atmosphere were to cease, eventually the earth would come to equilibrium at a new higher temperature satisfying Eq. (5.21).

Analysis of the exchange and transfer of long-wave radiation throughout the atmosphere is one of the main problems of physical meteorology but micrometeorologists are concerned primarily with the simpler problem of measuring or estimating fluxes at the surface. The upward radiative flux **L**u from a surface can be measured with a radiometer or from a knowledge of the surface temperature and emissivity. The downward flux from the atmosphere **L**d can also be measured radiometrically, calculated from a knowledge of the temperature and water vapor distribution in the atmosphere, or estimated from empirical formulae.

1 Terrestrial Radiation from Cloudless Skies

The radiance of a cloudless sky in the long-wave spectrum (or the effective radiative temperature) is least at the zenith and greatest near the horizon. This variation is a direct consequence of the increase in the path length of water vapor and carbon dioxide, the main emitting gases. In general, more than half the radiant flux received at the ground from a cloudless atmosphere comes from gases in the lowest 100 m and roughly 90% from the lowest kilometer. Themagnitude of the flux received at the surface is therefore strongly determined by temperature gradients near the ground.

It is convenient to define the apparent emissivity of the atmosphere εa as the flux density of downward radiation divided by full radiation at air temperature Ta measured near the ground, i.e.

Ld = $\varepsilon a \zeta\, T\, 4$ a . (5.22)